R99-04

# Participation by the South Dakota School of Mines and Technology Armored T-28 Storm-Penetrating Aircraft in the Turbulence Characterization and Detection Program, June, 1999

Andrew G. Detwiler and Rand E. Feind

*Prepared for:*

Aviation Safety Program
NASA Langley Research Center
Hampton, Virginia 23681-2199

## TABLE OF CONTENTS



## List of Figures



## List of Tables

# 1. Introduction

The purpose of the Turbulence Characterization and Detection (TCAD) program was to gain a better understanding of the air motion characteristics associated with convective activity and to determine how turbulence associated with convective activity can be more reliably detected by airborne Doppler weather radar. The facilities deployed for the program included three instrumented research aircraft, two fixed S-band research weather Doppler radars (one of which also had dual-polarization capabilities), and a mobile meteorological sounding facility. Support for this program was provided by the National Aeronautics and Space Administration (NASA) Aviation Safety Program (AVSP), and by Allied Signal/Honeywell and Rockwell-Collins, two airborne weather radar manufacturers who were part of the study.

A Convair 580, operated by Allied Signal/Honeywell, and a Rockwell Sabreliner, operated by Rockwell-Collins, each carried research airborne Doppler weather radars as well as instrumentation for measuring aircraft response to turbulence. The armored T-28, as will be discussed more fully below, carried a complement of meteorological, aircraft motion, and microphysical instruments, and a suite of 6 electric field meters. The Pawnee and CHILL radars, operated by the Colorado State University (CSU) CHILL radar facility, were used as a dual-Doppler weather radar network providing storm surveillance for guiding operations and for post-analysis of storm characteristics. The Research Applications Program (RAP) at the National Center for Atmospheric Research (NCAR) carried out atmospheric soundings on demand to monitor the thermodynamic characteristics and wind profile in the storm environment, and provided forecasting and real-time radar interpretation for operations.

Operations were directed from the CHILL radar site northeast of Greeley, Colorado. See Figure 1. Aircraft were based at Ft. Collins-Loveland Regional Airport (FNL), in Loveland, Colorado, about 50 km due west of the CHILL radar site. The mobile sounding unit was deployed from the Foothills Laboratory of NCAR, on the northeast side of Boulder, Colorado.

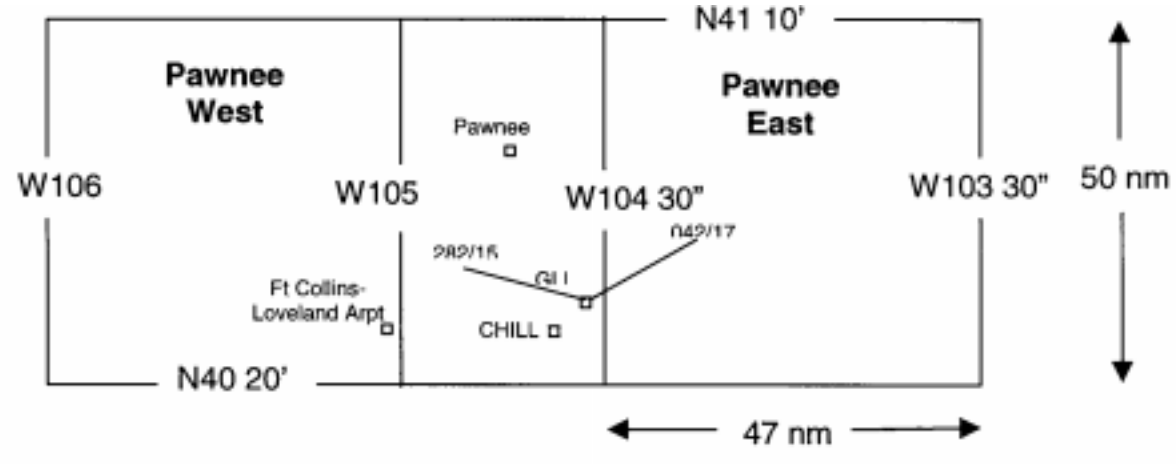


*Figure 1: A schematic map of the operations area, centered on the CSU-CHILL radar facility near Greeley, Colorado. Pawnee West and Pawnee East designate the two operations areas defined in cooperation with Denver operations center of the Federal Aviation Administration air traffic control system.*

A typical operation began with a sounding from the CHILL radar site at around 1100 MDT, and radar surveillance, beginning at about the same time, using the CHILL and Pawnee radars. When suitable convective activity developed, the aircraft were launched from FNL. They usually rendezvoused near the VORTAC (aircraft navigation beacon) near Gill, Colorado, a few kilometers northeast of the CHILL site. Under direction of an aircraft coordinator stationed in the CHILL operations trailer, the aircraft fell into a three-in-trail formation and proceeded to penetrate convective storm regions in this formation. The T-28 took the lead, with the others in-trail, one about 8 km and the other about 15 km or more behind the T-28. The weather radars on the two trailing aircraft scanned the T-28 environment as it penetrated the storms. The trailing aircraft followed the T-28 through if conditions were not too severe, or diverted around the severe regions and reformed with the T-28 on the other side of the storm. A typical T-28 flight level was FL 200 (20,000 ft or 6.1 km MSL) with the trailing aircraft 1000 ft above and below the T-28. A typical flight speed for the T-28 was 140 kts (72 m $s^{-1}$) indicated airspeed, or about 180 kts (95 m $s^{-1}$) true airspeed. Three to four coordinated runs were performed on most days, with the T-28 having to return to base after about ~90 minutes of flight. The other two aircraft often completed additional storm passes after the T-28 left the mission.

In some cases, the Sabreliner operated independently of the other two aircraft in order to sample higher altitude regions (up to FL 330) of storms while the Convair and T-28 sampled conditions near FL 200.

# 2. T-28 Operations Summary

## 2.1 Background

The T-28 crew for this project included:

Charles Summers – pilot/mechanic
Tom Root – pilot
Gary Johnson – hardware, instrumentation, and communications engineer
Rand Feind – software engineer
Andy Detwiler – facility scientist

The crew arrived on Tuesday, 1 June, and began to establish a base of operations at FNL and to install communications equipment at the CHILL radar site. The communications equipment included a VHF radio for air-ground communications and a ground station for the T-28 data telemetry system.

The first day of flight operations was Wednesday, 2 June, and the final day was Friday, 25 June. Operations were conducted 7 days a week, whenever suitable weather was present. It was a very active weather pattern, with convective weather suitable for flight operations in the project area on 15 days during this period. A summary of T-28 flights is given in Table 1.

By agreement, the time convention for all data recorded during the project was Universal Time (UT). Due to the fact that many flights straddled two different days in UT, and a problem in the T-28 telemetry display software that locked up the program when time increased to midnight UT then continued into the next day, T-28 data were recorded with the data acquisition system clock set to Mountain Daylight Time (MDT) and converted to UT in post-processing.

The T-28 telemetry system communicates using an UHF radio packet format with the ground station. If the aircraft unit loses contact with the ground station, data accumulate in a buffer and are dumped sequentially when contact is re-established. As the effective telemetry rate is relatively slow (4800 baud), the buffer can only be emptied at about twice real-time (2 seconds of backlogged data per 1 second of real time). As the aircraft was launched from a site 30 km east of the ground station, reliable contact typically was not obtained until the aircraft was airborne. In order to avoid backlogging a significant amount of data after the aircraft was first started, then taxied around the airport before it took off (often about 15 minutes), the data system was not started until the aircraft was in the air and in immediate contact with the ground station at the CHILL site.

| Table 1. T-28 Flights Conducted During TCAD | | | | | | |
|---|---|---|---|---|---|---|
| *Date* | *T-28 Flt. No.* | *Project Flt. No.* | *No. Hours* | *Type Mission* | *Location* | *Pilot* |
| 05-24 | 722 | | 1.6 | Test Flight | RAP | CS |
| 06-01 | 723 | | 1.8 | Ferry RAP-FNL | RAP | TR |
| 06-02 | 724 | | 1.8 | Wx Research | FNL | TR |
| 06-05 | 725 | 1 | 1.9 | Wx Research | FNL | TR |
| 06-09 | 726 | 3 | 2.0 | Wx Research | FNL | CS |
| 06-10 | 727 | 4 | 1.2 | Wx Research | FNL | CS |
| 06-11 | 728 | 5 | 1.8 | Wx Research | FNL | CS |
| 06-11 | 729 | 6 | 2.1 | Wx Research | FNL | CS |
| 06-12 | 730 | 7 | 1.8 | Wx Research | FNL | CS |
| 06-14 | 731 | 8 | 2.1 | Wx Research | FNL | TR |
| 06-17 | 732 | 10 | 2.0 | Wx Research | FNL | TR |
| 06-18 | 733 | 11 | 1.9 | Wx Research | FNL | TR |
| 06-19 | 734 | 13 | 2.1 | Wx Research | FNL | TR |
| 06-20 | 735 | 14 | 2.0 | Wx Research | FNL | TR |
| 06-21 | 736 | 16 | 1.8 | Wx Research | FNL | CS |
| 06-22 | 737 | 18 | 2.0 | Wx Research | FNL | CS |
| 06-25 | 738 | 20 | 1.4 | Ferry FNL-RAP | FNL | CS |
| | | | | | | |
| | | 31.3 hours | | | | |
| | | | | | | |
| 17 Total Flights<br>14 Total Weather Research Flights | | | | | | |

Time on the T-28 data acquisition system is maintained by an internal time chip in the acquisition computer. It is not slaved in real-time to a time standard. The time on the computer's clock was set each day to either the global positioning system time or to the CHILL radar computer time (which itself was set to the National Institutes of Science and Technology WWV time signal). It was discovered during this project that each time the data acquisition computer is booted, the computer's clock loses about 2 seconds. Typically the computer was booted once on the ramp just after engine startup to ensure that everything was working properly, then shut down, then re-booted in the air after take-off as the mission began. If the clock had

been set to an accurate source of time in the morning during system check-out, it would typically be about 4 seconds behind this standard once the data system was started for the second time. Time hacks performed during the mission, comparing aircraft time to radar time, showed that negligible time (to within a fraction of a second) was lost or gained during a flight, once the system started, but that often the T-28 data system time was 2 to 4 seconds behind the radar computer time.

A second source of time is the clock on the on-board video recorder. This time is derived from a clock chip within the recorder and was set in the same way as the data system time. When available, any information concerning the relationship between data system time, video recorder time, and CHILL time is provided below in the narrative summary of each day's flight.

A narrative follows of significant events occurring on each T-28 flight. As the data system was not started until after take-off, take-off time is estimated as 5 minutes prior to the time of the first recorded data.

## 2.2 Daily Operations

**2 June**
**T-28 Flt 724**
**Project Flt 1**
**T.O. ~21:25 UT**
**R.T.B. 23:03 UT**

A clear-air test flight was undertaken for testing operational procedures and coordination with other project aircraft. Small convective cells were nearby, but were not targeted. Poor telemetry reception to the northeast was traced to interference from the UHF wind profiler located next to the CHILL radar, north and east of the T-28 telemetry antenna. A pattern of working with ATC developed that was followed for most subsequent flights. Project aircraft rendezvoused near the Gill VORTAC in order to link up into a flight of 3. Experience on this flight suggested that the T-28 should extend ~10 mi beyond a target storm before turning to make another pass, in order to allow trailing aircraft to clear the storm, extend out, turn, and fall in behind to archive radar data on the subsequent pass. Pilots suggested that they could select specific penetration paths once given a general target. Rockwell-Collins and Allied Signal crews could pass course-correction guidance to the T-28 based on their onboard radar displays. All aircraft went under a small convective cell near the end of the flight and encountered negligible turbulence.

**5 June**
**T-28 Flt 725**
**Project Flt 3**
**T.O. ~19:50 UT**
**R.T.B. 21:26 UT**

Thunderstorm cells producing up to heavy precipitation and pea-size graupel, and up to moderate turbulence, were studied. Four coordinated passes involving all 3 project aircraft were

completed. The last pass was characterized by the most noticeable turbulence (~21:04 – pilot comments “rough ride”).

A brief steep descent, accompanied by an accelerometer spike, at 20:57, was pilot-induced.

The T-28 data system clock was 4 s behind GPS time. The T-28 video clock was 2 s behind GPS time. The output of the rate-of-climb indicator was bad. Small disparities are noted between the two pressure transducers, and also between the two temperature sensors. Static pressure #1 and the Rosemount temperature sensor are the more reliable.

**9 June**
**T-28 Flt 726**
**Project Flt 4**
**T.O. ~23:25 UT**
**R.T.B. ~ 01:05 UT**

Five coordinated runs involving the 3 aircraft were completed in small thunderstorm cells producing lightning, small hail, heavy precipitation, and moderate updrafts. Pilot reports indicated up to moderate turbulence.

**10 June**
**T-28 Flt 727**
**Project Flt 5**
**T.O. ~22:30 UT**
**R.T.B. 23:05 UT**

A severe hailstorm moved over DIA and gave the ATC controllers so much trouble that they cancelled the first attempt to launch the project aircraft to work convective cells within the project area. It actually hailed on the T-28 as it idled at the end of the FNL runway waiting for permission to launch, with hailstones up to marble size. A second launch request was granted, but just after the aircraft got organized into a flight and completed a first pass through a small dying convective cell, ATC requested a return-to-base due to excessive controller workload caused by the severe storm moving east from DIA.

**11 June**
**T-28 Flt 728**
**Project Flt 6**
**T.O. ~20:15 UT**
**R.T.B. 21:45 UT**

In the first flight on this day, the aircraft worked a storm ~60 km north of the CHILL radar. Four coordinated runs involving all 3 aircraft were completed. The T-28 encountered moderate to heavy turbulence, heavy icing, lightning, and strong updrafts on 4 runs. It also intercepted a vigorous turret on the way back to FNL.

Data system time and video time agree to within 1 s.

**T-28 Flt 729**
**Project Flt 7**
**T.O. ~23:15 UT**
**R.T.B. 01:01 UT**

The second mission of the day was focussed on multicellular storms less than 20 km north of the CHILL radar, moving northeastward during the mission. Three 3-aircraft coordinated runs were completed. The portions of these storms penetrated by the T-28 were more vigorous, more turbulent, and contained more hail than was encountered during penetrations on the first mission of the day.

The video clock was 4 s ahead of the data system clock. It is inferred that the data system clock was ~4 s behind UT. The cloud liquid water sensor was damaged by hail at 00:22:51 UT and no data were obtained from it for the remainder of the flight.

**12 June**
**T-28 Flt 730**
**Project Flt 8**
**T.O. ~20:15 UT**
**R.T.B. 21:43 UT**

The project aircraft worked storms 40 – 60 km east of CHILL. Four coordinated runs were accomplished involving all 3 aircraft. The T-28 encountered light turbulence, light icing, modest updrafts, and occasional lightning.

**14 June**
**T-28 Flt 731**
**Project Flt 10**
**T.O. 20:20 UT**
**R.T.B. 22:04 UT**

On this day the aircraft split into 2 separate missions, with the Convair and T-28 coordinating in passes near 20,000 ft MSL, while the Sabreliner operated near 35,000 ft. The mission focussed on a line of convective cells stretching north from the CHILL to the Colorado/Wyoming state line. Six coordinated runs were completed. Vigorous, very buoyant updrafts, moderate-to-heavy turbulence, and heavy precipitation were encountered by the T-28. Hail was not encountered.

The first pass was the most vigorous. The pilot reported cockpit accelerometer readings of up to 4 g's, although the peak vertical acceleration recorded was 0.7 g. Unfortunately, the de-icing circuit was inadvertently left off during the first pass, causing loss of data from the cloud water sensor and the research pitot. Loss of the pitot led to problems with any parameter or instrument requiring airspeed information. This includes our estimates of turbulent eddy

dissipation rate, updraft, and droplet and particle concentrations recorded by the PMS 2D-C and FSSP probes.

A big spike in calculated turbulence at 21:26:50 is an artifact caused by abrupt pilot action.

The data system clock was behind the CHILL clock by 2 sec, and behind the video clock by 4 sec.

**17 June**
**T-28 Flt 732**
**Project Flt 11**
**T.O. 22:15 UT**
**R.T.B. 00:04 UT**

The aircraft worked in a region with vigorous storms from 10 km to 40 km northeast of CHILL. Again, the aircraft split into 2 flights, with the Convair/T-28 flight focussed on the 20,000 ft flight level, and Sabreliner working higher at 28,000 ft. The T-28 pilot reported turbulence up to severe, with updrafts exceeding 3000 ft/min (~15 m/s) in clouds penetrated while circling near the Gill VORTAC to rendezvous with the Convair. Light-to-moderate turbulence with heavy precipitation was encountered during 3 coordinated passes. Severe convection was encountered again on the return-to-base after breaking off coordination with the Convair.

The cloud liquid water sensor was lost at 23:10 due to encounter with hail. The data system clock was 2 sec behind the CHILL computer clock. The video clock was 1 sec ahead of the data system clock.

**18 June**
**T-28 Flt 733**
**Project Flt 13**
**T.O. 20:40 UT**
**R.T.B. 22:18 UT**

The 3 project aircraft coordinated on passes through the upper portions of towering cumulus congestus clouds. Five coordinated runs were accomplished. Negligible to light turbulence, light icing, and light precipitation were encountered.

**19 June**
**T-28 Flt 734**
**Project Flt 14**
**T.O. 20:40 UT**
**R.T.B. 22:25 UT**

The 3 project aircraft coordinated on 5 runs. All 3 began in a coordinated flight near the 20,000 ft level, then the Sabreliner split away and began to work at higher altitudes. The flight began with a pass through mountain thunderstorms about 70 km west of CHILL. Then the focus of the flight became a large storm about 70 km north northwest of CHILL, near the Colorado/Wyoming state line. Light-to-moderate turbulence, moderate updrafts, up to heavy precipitation, and lightning were encountered by the T-28.

The T-28 data system clock was 4 sec behind CHILL computer clock.

**20 June**
**T-28 Flt 735**
**Project Flt 16**
**T.O. 22:05 UT**
**R.T.B. 23:54 UT**

The aircraft worked several vigorous thunderstorms from 60 to 100 km north northwest of CHILL, around the Colorado/Wyoming state line. Light-to-moderate turbulence, vigorous updrafts, icing, marble-size hail, and heavy precipitation were encountered.

**21 June**
**T-28 Flt 736**
**Project Flt 18**
**T.O. 21:53 UT**
**R.T.B. 23:28 UT**

The aircraft split into 2 flights, with the T-28 and Convair working the 20,000 ft flight level and the Sabreliner working above. Three coordinated Convair/T-28 runs were completed. The targets were some relatively weak convective cells over the Front Range, moving eastward during the mission. Generally light turbulence and light icing were encountered. The mission ended with the aircraft landing at FNL in rain.

**22 June**
**T-28 Flt 737**
**Project Flt 20**
**T.O. 20:52 UT**
**R.T.B. 22:35 UT**

The aircraft worked a line of high-based convection 40 to 80 km east of CHILL, associated with a front moving eastward at ~80 km/hr during the flight. The Sabreliner worked independently of the Convair and T-28. The Convair/T-28 mission included 4 coordinated runs.

Light to moderate turbulence and icing were encountered. Moderate turbulence was encountered frequently on this flight despite the relatively modest updrafts at flight level. High westerly winds aloft resulted in groundspeeds of 240 kts on the early eastward legs. Later in the flight, after the front got further east, winds aloft were weaker.

The flight was terminated when the T-28 ran out of anti-icing alcohol for its propeller, and the Convair lost its TCAS. Data collection was terminated at 22:18 UT, about 15 min prior to landing.

## 3. Data Summary

A summary of selected pass-by-pass statistics for all research flights is provided in Table 2. The beginning and end of a pass correspond to major cloud boundaries. The information contained in this table includes:

**Flt. No.** – A serial flight number for T-28 flights. The first flight in the series was in 1972. Under the flight number is the last name of the pilot on that flight.

**Date** – mm/dd/yy

**Run** – During operations, coordinated formation flight legs were given run numbers. There may be more than one cloud episode during one run, and there may be cloud episodes listed outside the time of the runs. The definition of the beginning and ending of one cloud episode is somewhat subjective, especially in regions containing much cloud and cloud debris.

**Begin, End** – Beginning and ending times of cloud episode, in UT

**Avg. Z** – Average altitude above sea level during the episode (m)

**Avg. T** – Average temperature during the episode (C)

**Max LWC** – Maximum cloud water concentration, based on the DMT liquid water probe ($g\ m^{-3}$)

**FSSP Max #** – Maximum cloud droplet concentration, based on the FSSP ($\#\ cm^{-3}$)

**Max Precip** – Maximum precipitation particle concentration, based on 2D-C ($\#\ \ell^{-1}$)

**Max W+** – Maximum updraft speed ($m\ s^{-1}$)

**Max Turb** – Maximum turbulent energy dissipation rate ($cm^{2/3}\ s^{-1}$)

**Max accel** – Absolute magnitude of maximum vertical acceleration (g)

**PIREP** – relevant pilot comments, if noted in real-time by observers on the ground listening to air-ground communication, or if noted during preliminary review of the flight video. If something is not mentioned here, it does not necessarily mean it didn't occur. Further review of the audio track of the flight video may reveal additional information.

This table is intended as a preliminary aid in sorting through the flights for data of interest for one purpose or another. Obvious artifacts have been filtered out of the table, but additional, more-detailed analyses may reveal the need for further revision.

## Table 2: Turbulence Project Data Summary

| T-28 Flt No. | Date | Run | Begin [UT] | End [UT] | Avg Z [m] | Avg T [C] | Max LWC [g $cm^{-3}$] | FSSP Max [# $cm^{-3}$] | Max Prcp [# $\ell^{-1}$] | Max W+ [m $s^{-1}$] | Max Turb [$cm^{2/3}$ $s^{-1}$] | Max accel [g] | PIREP |
|---|---|---|---|---|---|---|---|---|---|---|---|---|---|
| 725 | 6/5/1999 | 1 | 20:29:57 | 20:35:50 | 6080 | -18.9 | 0.1 | 140 | 687 | 5 | 8.3 | 1.6 | |
| Root | | 2 | 20:36:10 | 20:49:03 | 6058 | -19 | 0.4 | 378 | 818 | 6 | 5.8 | 1.9 | lgt/mod turb, carb icing |
| | | 3 | 20:50:10 | 20:53:28 | 6113 | -19 | 0.6 | 494 | 624 | 13 | 13.2 | 1.7 | lgt/mod turb |
| | | 4 | 20:54:01 | 21:01:30 | 6046 | -18 | 1 | 764 | 2001 | 13 | 15.9 | 2.3 | mod turb |
| 726 | 6/9/1999 | 1 | 23:46:33 | 23:49:59 | 5446 | -11 | 0.1 | 484 | 85 | 2 | 4.0 | 1.6 | one large accel spike ~174730; stick mvmnt? |
| Summers | | 2 | 23:56:41 | 23:59:42 | 5450 | -11 | 0.1 | 486 | 367 | 2 | 6.3 | 1.6 | ditto; ~175712 |
| | | 2 | 0:01:46 | 0:02:10 | 5437 | -12 | 0.2 | 368 | 11 | 1 | 3.3 | 1.5 | |
| | | 3 | 0:08:34 | 0:11:25 | 5454 | -11 | 0.8 | 558 | 757 | 12 | 13.8 | 1.5 | |
| | | 4 | 0:23:30 | 0:32:35 | 4509 | -5 | 0.6 | 671 | 302 | 7 | 10.9 | 1.9 | mdt turb |
| | | 5 | 0:33:58 | 0:39:57 | 4504 | -5 | 0.7 | 688 | 460 | 6 | 11.9 | 2.1 | |
| 727 | 6/10/1999 | 1 | 22:53:00 | 22:58:00 | 5383 | -12 | 0.2 | 630 | 381 | 7 | 4.8 | 1.4 | smooth |
| Summers | | | | | | | | | | | | | |
| 728 | 6/11/1999 | 1 | 20:34:57 | 20:36:32 | 5382 | -11 | 1.2 | 844 | 235 | 9 | 9.7 | 1.7 | lgt turb outside cloud;initially rough on entry;carb icing |
| Summers | | 2 | 20:48:10 | 20:52:32 | 5394 | -12 | 1.2 | 728 | 865 | 12 | 9.9 | 1.4 | initially smooth; then updraft/icing/ltng |
| | | 3 | 21:07:50 | 21:15:38 | 5390 | -13 | 0.9 | 703 | 1017 | 11 | 13.3 | 1.7 | strong up;ltng;hail |
| | | 4 | 21:20:29 | 21:29:20 | 5369 | -12 | 1.1 | 858 | 772 | 13 | 19.5 | 1.7 | ltng |
| 729 | 6/11/1999 | 1 | 23:53:44 | 23:55:50 | 4778 | -6 | 1 | 659 | 576 | 12 | 10.1 | 1.4 | ltng |
| Summers | | 1 | 23:59:00 | 0:00:32 | 4777 | -7 | 0.2 | 490 | 237 | 4 | 5.5 | 1.4 | smooth |
| | | 1 | 0:03:03 | 0:06:23 | 4766 | -8 | 0.4 | 271 | 448 | 4 | 15.2 | 1.4 | |

**Table 2: Turbulence Project Data Summary, continued**

| T-28 Flt No. | Date | Run | Begin [UT] | End [UT] | Avg Z [m] | Avg T [C] | Max LWC [g $cm^{-3}$] | FSSP Max [# $cm^{-3}$] | Max Prcp [# $\ell^{-1}$] | Max W+ [m $s^{-1}$] | Max Turb [$cm^{2/3}$ $s^{-1}$] | Max accel [g] | PIREP |
|---|---|---|---|---|---|---|---|---|---|---|---|---|---|
| | | 2 | 0:10:28 | 0:12:34 | 4771 | -8 | 0.6 | 578 | 68 | 3 | 5.8 | 1.4 | |
| | | 2 | 0:13:49 | 0:27:00 | 4771 | -8 | 1.2 | 763 | 885 | 17 | 15.2 | 1.9 | updraft; turb; soft hail at end in clear |
| | | 3 | 0:36:50 | 0:45:16 | 5 | -10 | 1.1 | 653 | 507 | 15 | 11.4 | 1.4 | icing |
| | | unofficial | 0:57:26 | 0:59:26 | 1927 | 13 | 0 | 0 | 38 | 7 | 6.2 | 1.4 | |
| 730 | 6/12/1999 | 1 | 20:49:39 | 20:51:25 | 6660 | -21 | 0.8 | 524 | 918 | 9 | 11.7 | 1.6 | |
| Summers | | 2 | 21:01:23 | 21:02:01 | 6649 | -21 | 0 | 16 | 168 | 5 | 3.1 | 1.5 | |
| | | 2 | 21:04:09 | 21:06:49 | 6657 | -22 | 0.1 | 176 | 1297 | 5 | 5.4 | 1.5 | |
| | | 3 | 21:17:40 | 21:19:54 | 6070 | -17 | 0.7 | 614 | 1510 | 12 | 10.0 | 1.5 | |
| | | 4 | 21:23:19 | 21:30:14 | 6052 | -17 | 0.1 | 168 | 1053 | 5 | 10.2 | 1.5 | ltng; smooth ride |
| 731 | 6/14/1999 | 1 | 20:50:00 | 20:57:00 | 6191 | -12 | 2+ | 800 | 2000 | 40+ | 12+ | 1.7 | pitot iced; no DMT liq water |
| Root | | 2 | 21:01:00 | 21:10:00 | 6400 | -18 | 1.2 | 510 | 1589 | 22 | 9.7 | 1.7 | initially smooth; updraft at end |
| | | 3 | 21:11:00 | 21:19:00 | 6430 | -17 | 1.3 | 534 | 1789 | 21 | 12.0 | 1.4 | |
| | | 4 | 21:20:00 | 21:27:00 | 6398 | -17 | 0.9 | 475 | 2275 | 18 | 14.6 | 1.6 | |
| | | 5 | 21:36:00 | 21:42:00 | 6354 | -17 | 1.1 | 549 | 1180 | 15 | 10.4 | 1.5 | |
| | | 6 | 21:46:00 | 21:50:00 | 6383 | -17 | 0.1 | 52 | 1108 | 5 | 6.6 | 1.3 | |
| 732 | 6/17/1999 | unofficial | 22:26:09 | 22:26:56 | 3449 | 5 | 0.3 | 845 | 38 | 4 | 7.3 | 1.3 | near cloud base; climbing |
| Root | | unofficial | 22:26:58 | 22:27:02 | 3835 | 2 | 0.1 | 754 | 9 | 4 | 4.5 | 0.8 | climbing |
| | | unofficial | 22:27:43 | 22:28:31 | 4152 | 0 | 0.6 | 691 | 60 | 7 | 5.8 | 1.3 | climbing |
| | | unofficial | 22:30:25 | 22:34:57 | 5240 | -9 | 0.3 | 434 | 67 | 3 | 12.0 | 1.3 | climbing through series of brief cloud encounters,~constant alt. |
| | | unofficial | 22:35:02 | 22:36:06 | 5612 | -10 | 0.3 | 330 | 24 | 2 | 3.9 | 1.2 | brief cloud encounter only 163500-163506; restart climb |

**Table 2: Turbulence Project Data Summary, continued**

| T-28 Flt No. | Date | Run | Begin [UT] | End [UT] | Avg Z [m] | Avg T [C] | Max LWC [g $cm^{-3}$] | FSSP Max [# $cm^{-3}$] | Max Prcp [# $\ell^{-1}$] | Max W+ [m $s^{-1}$] | Max Turb [$cm^{2/3}$ $s^{-1}$] | Max accel [g] | PIREP |
|---|---|---|---|---|---|---|---|---|---|---|---|---|---|
| | | unofficial | 22:36:16 | 22:36:37 | 5865 | -11 | 0.7 | 656 | 52 | 5 | 7.4 | 1.3 | climbing again |
| | | unofficial | 22:36:44 | 22:38:11 | 6021 | -13 | 0.8 | 638 | 99 | 7 | 10.2 | 1.6 | climbing |
| | | unofficial | 22:39:34 | 22:40:08 | 6477 | -16 | 0.6 | 436 | 52 | 4 | 6.5 | 1.2 | fairly level |
| | | unofficial | 22:46:20 | 22:46:37 | 7028 | -19.9 | 0.8 | 528.1 | 34 | 5 | 6 | 1.3 | nearly thru top of new cell NW of main storm |
| | | unofficial | 22:48:24 | 22:48:50 | 6836 | -18 | 0.7 | 480 | 6 | 0 | 10.4 | 1.4 | |
| | | 1 | 22:51:17 | 22:58:25 | 6682 | -17 | 1 | 691 | 272 | 15 | 7.7 | 1.3 | Run 1 started 165600; after turn within this period. Major updraft starts 165715 |
| | | 1 | 23:00:24 | 23:03:38 | 6698 | -18 | 0.1 | 14 | 118 | 2 | 4.5 | 1.3 | turn near end of period |
| | | unofficial | 23:04:33 | 23:05:09 | 6692 | -18 | 0 | 0 | 17 | M | 2.9 | 1.2 | in turn |
| | | 2 | 23:07:53 | 23:15:55 | 6530 | -16 | 1.8 | 445 | 2915 | 16 | 17.7 | 1.7 | strong up 170930-171030 |
| | | unofficial | 23:26:51 | 23:31:08 | 6063 | -13 | 0.2 | 196 | 153 | M | 3.8 | 1.3 | in turn for part of period |
| | | 3 | 23:32:18 | 23:39:48 | 6099 | -13 | 1.5 | 554 | 1365 | 11 | 14.7 | 1.5 | more convective at end of pass |
| | | unofficial | 23:46:04 | 23:54:56 | 3128 | 5 M | | 478 | 33 M | | 8.9 | 1.8 | descending; rough ride |
| | | | | 6:00:00 | | | | | | | | | |
| 733 | 6/18/1999 | 1 | 21:16:13 | 21:21:27 | 6664 | -17 | 0 | 0 | 0 | 0 | 2.0 | 1.2 | over top of TCu; turn at end of period |
| Root | | 2 | 21:23:16 | 21:23:27 | 6602 | -17 | 0.7 | 379 | 8 | 0 | 2.3 | 1.1 | just in tops |
| | | 3 | 21:37:19 | 21:38:36 | 6076 | -14 | 1 | 709 | 18 | 8 | 9.8 | 1.2 | hard-looking turret |
| | | 4 | 21:49:23 | 21:50:16 | 6048 | -13 | 0.7 | 480 | 95 | 7 | 8.0 | 1.4 | turn near end of period |
| | | 5 | 21:56:48 | 21:58:31 | 5092 | -7 | 0.5 | 471 | 97 | 5 | 4.2 | 1.4 | |
| | | 5 | 21:59:42 | 22:01:48 | 5085 | -7 | 0.7 | 660 | 49 | 6 | 4.8 | 1.4 | |
| | | 5 | 22:03:16 | 22:03:20 | 5088 | -7 | 0.3 | 354 | 2 | 3 | 2.7 | 1.1 | |
| | | 5 | 22:03:58 | 22:05:40 | 5079 | -7 | 0.5 | 526 | 107 | 0 | 2.7 | 1.2 | |
| | | 5 | 22:06:59 | 22:07:31 | 5062 | -7 | 0.2 | 475 | 48 | 0 | 2.0 | 1.1 | |

**Table 2: Turbulence Project Data Summary, continued**

| T-28 Flt No. | Date | Run | Begin [UT] | End [UT] | Avg Z [m] | Avg T [C] | Max LWC [g $cm^{-3}$] | FSSP Max [# $cm^{-3}$] | Max Prcp [# $\ell^{-1}$] | Max W+ [m $s^{-1}$] | Max Turb [$cm^{2/3}$ $s^{-1}$] | Max accel [g] | PIREP |
|---|---|---|---|---|---|---|---|---|---|---|---|---|---|
| 734 | 6/19/1999 | unofficial | 21:06:23 | 21:07:02 | 5782 | -12 | 0.2 | 425 | 1 | 0 | 2.3 | 1.2 | |
| Root | | 1 | 21:08:52 | 21:15:04 | 5754 | -11 | 0.4 | 568 | 527 | 2 | 9.2 | 1.5 | smooth ride |
| | | 1 | 21:15:17 | 21:16:17 | 5757 | -11 | 0.1 | 367 | 105 | M | 3.1 | 1.2 | in turn |
| | | 2 | 21:20:09 | 21:24:38 | 5741 | -11 | 0.3 | 534 | 677 | 6 | 3.8 | 1.4 | coming out of turn at beginning; lgt turb, lgt precip |
| | | unofficial | 21:25:44 | 21:26:47 | 5727 | -13 | 0.2 | 527 | 1 | 3 | 3.3 | 1.5 | course correction in middle |
| | | 3 | 21:32:16 | 21:41:04 | 5758 | -12 | 0.9 | 697 | 241 | 17 | 7.9 | 1.4 | 2 vigorous updrafts; lgt/mod turb |
| | | 4 | 21:46:00 | 21:52:38 | 5760 | -12 | 0.2 | 284 | 1037 | 3 | 13.1 | 1.4 | lgt turb in clear after end |
| | | 5 | 21:58:16 | 22:06:33 | 5745 | -10 | 0.1 | 486 | 1169 | 6 | 9.3 | 1.4 | lgt turb; rougher ride after this on way home |
| 735 | 6/20/1999 | 1 | 22:41:43 | 22:47:54 | 6058 | -13 | 0.4 | 537 | 575 | 9 | 9.0 | 1.3 | lgt/mod turb, snow, icing; 4 convective elements |
| Root | | 2 | 22:53:32 | 22:59:39 | 6067 | -13 | 0.7 | 509 | 858 | 16 | 7.6 | 1.5 | snow, graupel, lgt turb |
| | | 3 | 23:07:14 | 23:11:34 | 6098 | -13 | 0.8 | 706 | 1297 | 9 | 8.0 | 1.5 | multiple updrafts, lgt/mod turb; icing |
| | | 4 | 23:17:58 | 23:27:38 | 6060 | -14 | 1.1 | 757 | 1794 | 20 | 8.1 | 1.4 | marble-size hail; mod turb |
| | | 5 | 23:30:27 | 23:36:17 | 6067 | -13 | 1 | 726 | 1158 | 13 | 10.3 | 1.4 | mod turb; add'l precip on way home |
| 736 | 6/21/1999 | 1 | 22:22:58 | 22:30:00 | 5458 | -8 | 0.3 | 455 | 1083 | 6 | 6.2 | 1.4 | ltng,updraft,lgt turb |
| Summers | | 2 | 22:44:56 | 22:55:56 | 5434 | -8 | 0.1 | 315 | 379 | 5 | 8.1 | 1.5 | lgt turb; glitches in StPr produce artificial updraft spikes |
| | | 3 | 22:59:28 | 23:02:52 | 5447 | -9 | 0.5 | 405 | 554 | 6 | 5.9 | 1.5 | lgt chop; RFT and StPr noisy |
| 737 | 6/22/1999 | 1 | 21:14:26 | 21:21:17 | 5742 | -11 | 0.4 | 704 | 664 | 8 | 7.7 | 1.4 | mod turb/lgt ice |
| Summers | | unofficial | 21:26:18 | 21:26:59 | 5735 | -12 | 0.2 | 618 | 23 | 0 | 6.0 | 1.6 | in small buildup |
| | | 2 | 21:29:54 | 21:37:01 | 5740 | -11 | 0.4 | 687 | 947 | 6 | 10.1 | 1.6 | lgt turb |
| | | 3 | 21:44:23 | 21:54:07 | 5781 | -11 | 0.5 | 753 | 246 | 8 | 10.7 | 1.6 | lgt chop outside cloud on way in, also in cloud |
| | | 4 | 21:59:27 | 22:09:26 | 5771 | -11 | 0.6 | 825 | 581 | 8 | 9.5 | 1.9 | at beginning of run, T-28 looped once to increase separation from Convair |

# 4. Instrumentation

The instrumentation carried by the T-28 during this project is tabulated in Appendix A.

## 4.1 Aircraft Motion

Aircraft track is provided by a Trimble 2000 GPS unit. Position is updated each second when a sufficient number of satellites are in contact. Latitude, longitude, and altitude are recorded. Prior comparisons to positions obtained from the FAA ARTCC system show reasonable agreement, and that generally, when position relative to a known reference point is checked, GPS positions are more accurate. The GPS position data are recorded with the T-28 data stream. GPS time is recorded for only the last 2 flights.

Airspeed is computed using dynamic pressure obtained from a pitot-static probe under the right wing, and static pressure obtained from a side-facing pressure port on the rear fuselage. The pressure transducers, two dynamic and two static, are all mounted in the rear fuselage. The roughly 5 m long pressure line from the under-wing pitot port to the transducers effectively damps out frequencies higher than a few Hz in the dynamic pressure signal. An example of a power spectrum of a short segment of dynamic pressure data is shown in Figure 2.

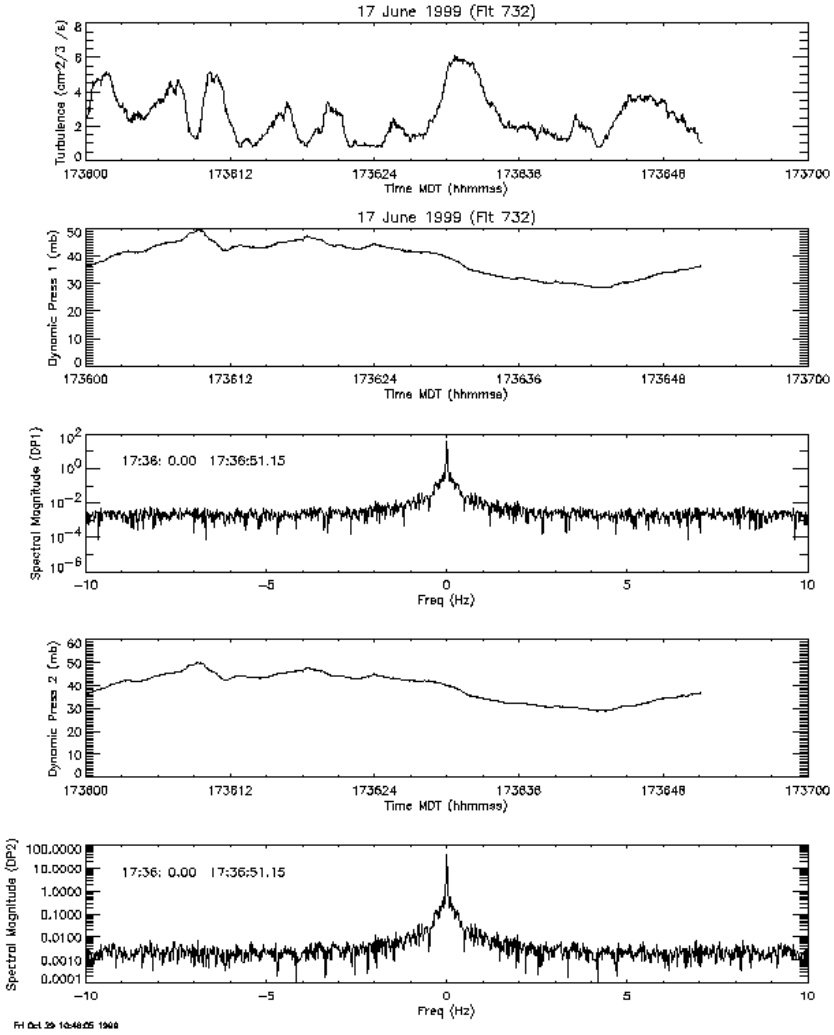


*Figure 2: Example showing 51 seconds (1024 pts at 20/sec) of estimated turbulent energy dissipation rate and output from the two dynamic pressure sensors in the T-28, on 17 June. The power spectra derived from the two pressure transducers roll off rapidly within 2 Hz. Dynamic pressure sensor No. 2 is noisier than sensor No. 1. Note that the time scale is in local time rather than UT.*

The static pressure signal is affected by noise due to radio-frequency (RF) interference when there is a cockpit radio transmission. The result is few-second-long pulses in the static pressure signal with an amplitude of a few hPa. An example of such pulses is shown in Figure 3. RF interferes also with the recorded interior temperature data (tag 121, Appendix B). Correlation in time between noise in interior temperature and in static pressure is a diagnostic for RF interference.

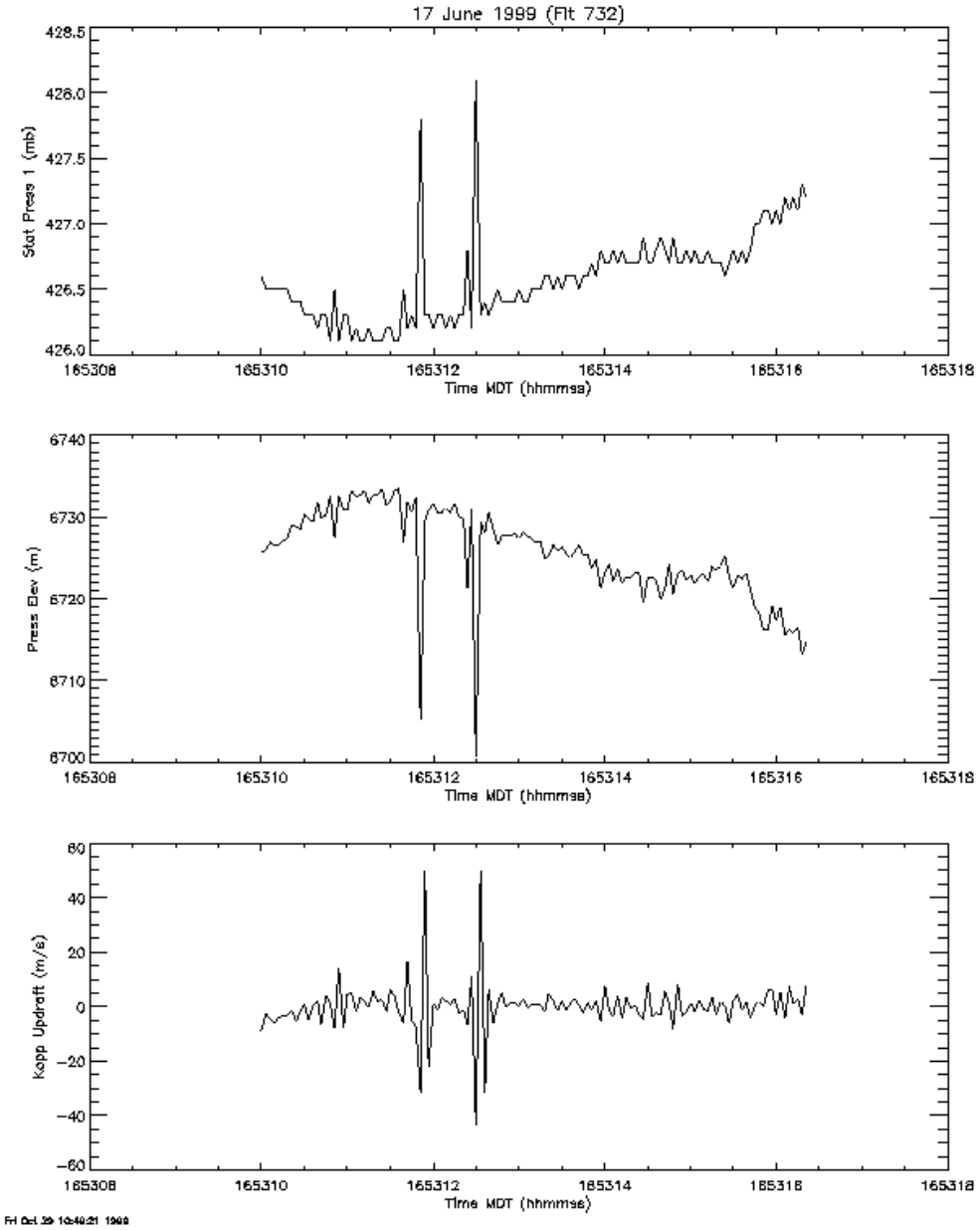


*Figure 3: An example from the flight on 17 June showing how radio frequency interference in the static pressure record introduces artifacts in the derived parameters pressure altitude and updraft. Note that the time scale is in local time rather than UT.*

The two dynamic pressure transducers perform similarly. The two static pressure transducers do not. The parameter we call "Static Pressure 2" (data tag number 104, appendix B) is generally much noisier than "Static Pressure 1" (data tag number 103, appendix B).

Two accelerometers were installed in the T-28 for this project. One is a Humphrey vertically-stabilized accelerometer, and the other a Crossbow Technologies 3-axis accelerometer fixed to the aircraft frame of reference. Both were mounted as close as possible to the aircraft center of gravity, behind the pilot's seat. Comparison of the readings from these instruments showed very good agreement in straight-and-level flight. Peak vertical accelerations were typically several times greater than peak horizontal accelerations on most passes. Examples of power spectra from a short segment of vertical acceleration data are shown in Figure 4, including data from both the vertically-stabilized Humphrey accelerometer as well as the unstabilized Crossbow accelerometer. The accelerometer spectra are even more sharply-peaked than the dynamic pressure spectra.

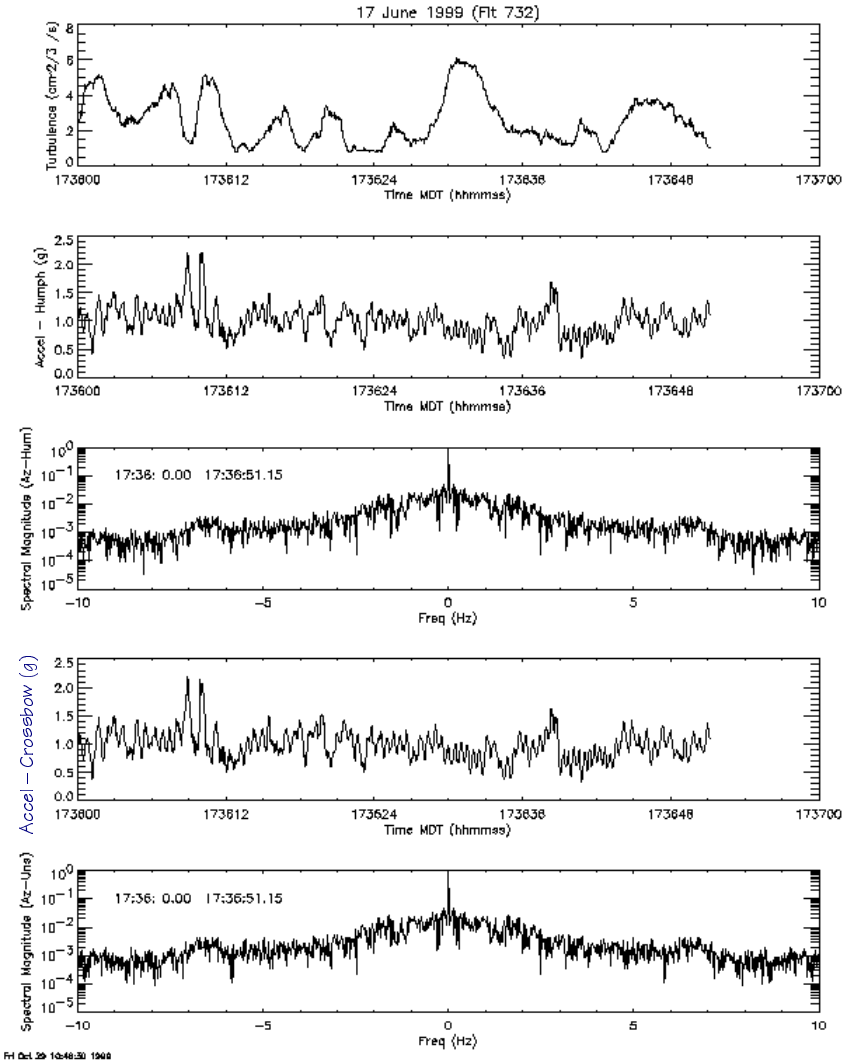


*Figure 4: For the same period as shown in Figure 2, turbulence and the vertical acceleration from the Humphrey vertically-stabilized accelerometer as well as the Crossbow unstabilized accelerometer are shown, along with their power spectra. The peak at DC is even sharper in the acceleration data than in the airspeed data.*

Manifold pressure is recorded, but no additional aeronautical parameters, such as throttle setting, engine RPM, aircraft control surface positions, etc., were recorded. Pitch and roll are obtained from the vertically-stabilized Humphrey accelerometer. There was no probe for angle-of-attack. Due to the fact that most T-28 data of interest were recorded during formation flying, when safety concerns require the pilot to carefully hold altitude, aircraft response to vertical gusts was often modified by pilot actions.

## 4.2 Meteorological and Microphysical Parameters

### 4.2.1 Temperature

Temperature is available from two sensors, mounted under the left wing. The fundamental sensing element in each probe is a platinum resistance element. The de-iced Rosemount sensor (data tag 106, Appendix B) is more stable and more accurate in dry air and in light icing conditions. It has a response time of approximately 1 second. The reverse-flow temperature sensor (data tag107, Appendix B) is designed to provide a measure of temperature unaffected by icing even in heavy icing conditions. It has a response time of approximately 4 seconds. It's response is more sensitive to variations in angle-of-attack, and to changes in airflow due to icing, than is the response of the Rosemount sensor, but relative variations in temperature from one region to another in moderate to heavy icing regions are better judged using the reverse-flow sensor. There is some RF-induced noise in the recorded reverse-flow temperature, with amplitude of fractions of a degree Celsius.

### 4.2.2 Vertical wind

Vertical wind is approximated using a simplified inversion of the aircraft equation of motion. (Kopp, 1985). The most important component of this estimate is the rate of change of aircraft pressure altitude, which is approximated as a centered difference, one second either side of the second at which the computed value is stored. The most simplifying approximation in the equation of motion is substituting pitch (which is measured on the T-28) for angle-of-attack (which is not measured). This approximation leads to an improvement in estimated vertical wind over that obtained using solely the rate-of-change of aircraft pressure altitude as a proxy for vertical wind, but is not as accurate as would be a similar calculation with a measured angle-of-attack.

The occasional appearance of RF-induced excursions in static pressure leads to corresponding excursions in computed pressure altitude, which in turn leads to artifacts in the vertical wind data series. These artifacts are easily recognized as up/down couplets with amplitude 20 m $s^{-1}$ or more, spread over a period of a few seconds. An example is shown in Figure 3.

### 4.2.3 Turbulence

Turbulent eddy dissipation rate is estimated using an algorithm developed by Sand (Sand *et al.* 1976), based on earlier work described in MacCready (1962). The basic principle is based on the spectral properties of homogeneous turbulence in the inertial subrange. A power spectrum of the fluctuations in true airspeed is computed using a running window 3.2 seconds in length. The estimate of power at any frequency can be related to the turbulent energy dissipation

rate assuming there is an inertial subrange spectral slope of –5/3. The power is computed at 32 discrete frequencies, the eddy dissipation rate is estimated independently based on each of the 32 frequencies, and a weighted average is taken. This average is used as the estimate of the turbulent energy dissipation rate. Sand *et al.* (1976) show some examples based on data obtained in thunderstorms by the T-28. While there are alternative, more sophisticated methods for estimating turbulent energy dissipation rate (e.g. Cornman *et al.*, 1993), this approach has been shown to produce estimates in qualitative agreement with T-28 pilot reports of turbulence.

Airspeed fluctuations can be qualitatively correlated with turbulence characteristics. Sand (1976) gives an empirical correlation between airspeed fluctuations and pilot-reported turbulence intensity in aircraft of the weight and speed class of the T-28:

| | |
|---|---|
| Light : | $2.5 – 7.5$ m $s^{-1}$ |
| Moderate: | $7.5 – 12.5$ m $s^{-1}$ |
| Severe: | $> 12.5$ m $s^{-1}$ |

### 4.2.4 Cloud Water

Two instruments on the T-28 provide information about cloud water. The Droplet Measurement Technologies (DMT) liquid water sensor is a heated coil for which heat loss can be correlated with cloud liquid water concentration. The Particle Measuring Systems, Inc. (PMS) Forward Scattering Spectrometer Probe (FSSP) is an optical, single-particle counter which provides droplet size spectra. Both performed well during the project, with generally good agreement between the DMT liquid water concentration and the liquid water concentration computed by integrating the FSSP spectra. During some penetrations high ice particle concentrations introduced some noise into the FSSP spectra. (See, e.g., Gardiner and Hallet, 1986.)

### 4.2.5 Precipitation

Cloud ice and small precipitation particles were imaged with a PMS optical array probe (OAP) providing two-dimensional shadow images of particles with a vertical window height of 0.8 mm (2D-C). This probe performed very well during the project.

Larger precipitation particles were imaged and counted by the custom-built optical array hail spectrometer, sensitive to particles between 0.9 mm and 12 cm in diameter. The automated counting and sizing circuitry includes only particles in the size range 4.5 mm to 4.5 cm. The probe performed well during the project, except during descent. It is not de-iced, and descent from cooler to warmer layers of the atmosphere caused condensation on the windows and loss of data.

Additional information on large particles can be inferred from the recorded audio signal from a small microphone mounted to the forward-facing cockpit windscreen. Hailstones hitting the wind screen produce audible signals. Mushy hailstones produce muffled sounds, while hard hailstones sound almost like a hammer hitting the windscreen.

## 5. Preliminary Data Survey

A comprehensive survey of the properties of convective storms in northeastern Colorado has been compiled in Knight and Squires (1982). The storms encountered during the TCAD Program spanned the range from towering cumulus to large thunderstorms. The properties of these storms were within the range of those surveyed in the work presented in Knight and Squires (1982).

A summary of pass-by-pass extreme values of selected parameters has been presented in Table 2. Based on these data, we briefly explore correlations between these extreme values. Due to the nature of the flight operations, it must be noted that in all likelihood, on most passes, the peak values encountered by the T-28 do not represent the peak values at its altitude in the storm, and most certainly not the peak values throughout the storm. The T-28 was often steered away from the highest reflectivity areas, and in most cases probably did not encounter either the maximum precipitation rates or the maximum up or down drafts. In most cases, the peak values of the different parameters were encountered at different times on a pass. Often, multiple up and downdrafts, precipitation cores, and turbulent regions were encountered within the same storm pass. Thus these summary statistics are merely qualitative indicators of storm structure and storm processes.

One expected correlation is between peak values of turbulent energy dissipation rate and peak values of updraft speeds. Whether one applies the conceptual model of the entraining jet, or the rising bubble, to represent an updraft, the shear along the edges of an updraft can be expected to generate eddies that then decay. The stronger is the updraft, the stronger is the shear. The stronger is the shear, the greater is the turbulence. Unless the updraft is subject to active entrainment, the most turbulent areas should be just outside the updraft, rather than centered within it. Figure 5 shows a close correlation between peak updraft magnitude encountered by the T-28, and peak turbulent energy dissipation rates.

Another expected correlation is between peak updraft speed and peak cloud liquid water concentration. Stronger updrafts tend to be broader, with less entrainment and thus higher cloud water concentration, occurring in the cores of stronger updrafts reaching the T-28 altitude. In addition, higher cloud water concentration is expected in younger fresher updrafts prior to the development of precipitation with subsequent cloud water scavenging and precipitation drag. Such a positive correlation between peak cloud water concentration and peak updraft magnitude is shown in Figure 6. Because of the two correlations shown in Figure 5 and 6, one would also expect peak turbulence and peak cloud water concentration to be well-correlated, as indeed is shown in Figure 7.

The correlation between peak values of vertical acceleration and of turbulent eddy dissipation rate is shown in Figure 8. Perhaps due to the effects of pilot-induced accelerations, the correlation is positive but noisy.

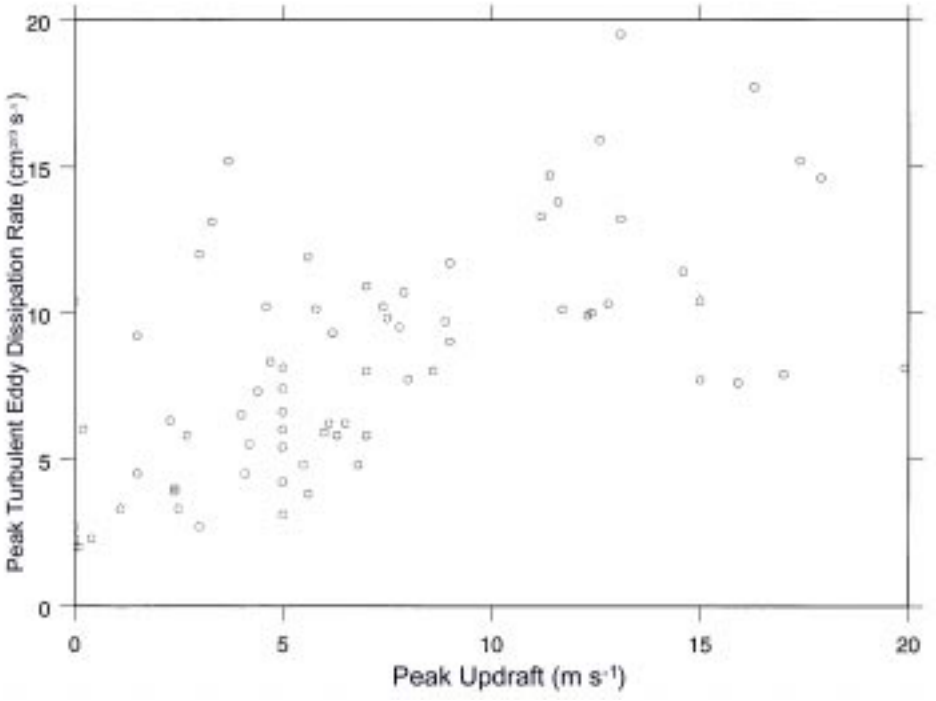


*Figure 5: Peak values of turbulent eddy dissipation rate and updraft for each pass designated in Table 2 are compared.*

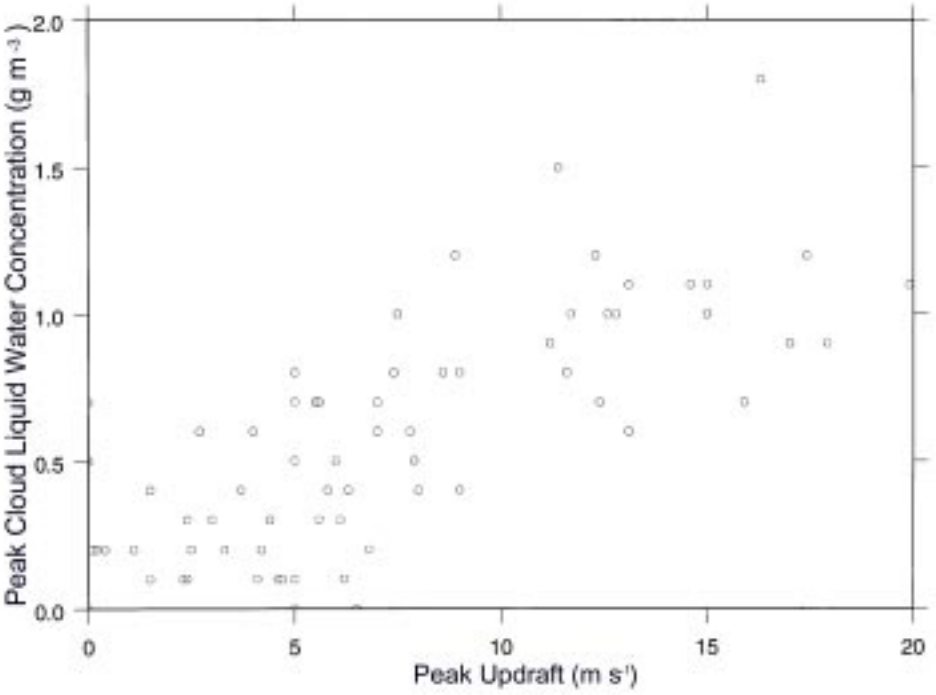


*Figure 6: Peak values of cloud water concentration and updraft for each pass designated in Table 2 are compared.*

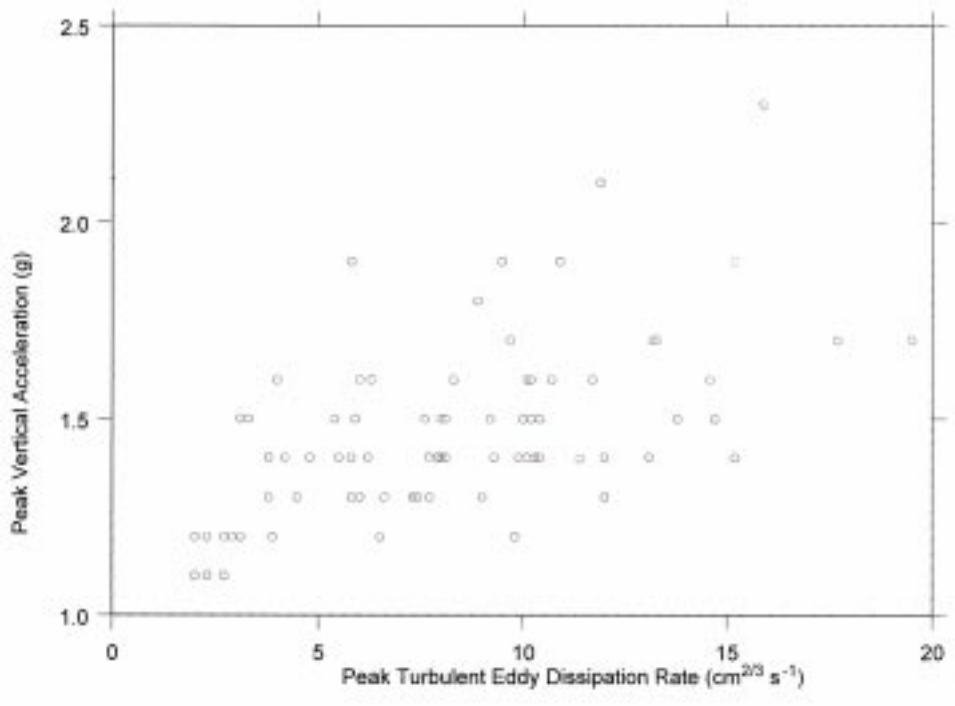


*Figure 7: Peak values of cloud liquid water concentration and turbulent eddy dissipation rate for each pass designated in Table 2 are compared.*

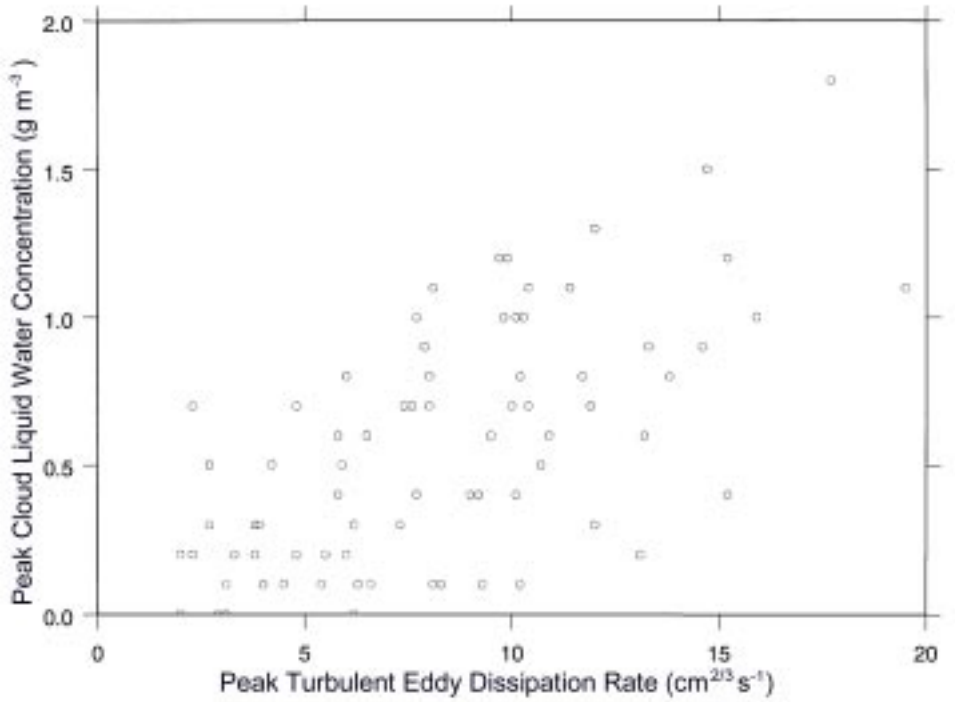


*Figure 8: Peak values of vertical acceleration and turbulent eddy dissipation rate for each pass designated in Table 2 are compared.*

Next, we examine detailed observations from two runs on the first flight on 11 June (T-28 Flight Number 728). In Figure 9 data are shown from Run 2, including updraft, cloud liquid water concentration, precipitation particle count rate, and turbulent eddy dissipation rate. The pass is from northwest-to-southeast through a storm to the northeast of CHILL. (See flight track in Appendix D.) A modest updraft with a peak magnitude of ~10 m $s^{-1}$ is shown. Significant cloud water concentration is associated only with the updraft, while precipitation is most concentrated on the flank of the updraft. Turbulence is episodic, with narrow peaks associated with abrupt changes in the updraft magnitude.

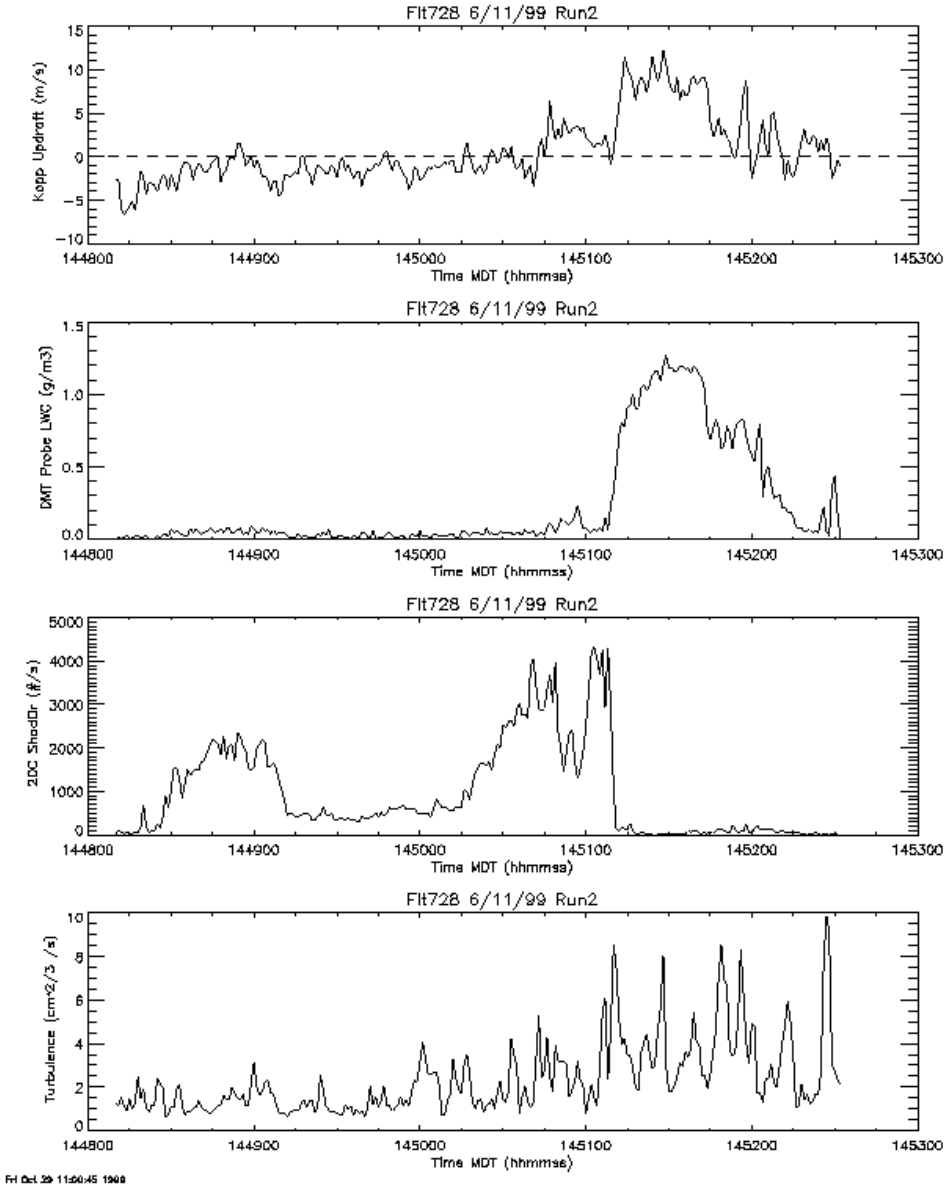


*Figure 9: Updraft, cloud water concentration, the 2D-C precipitation particle count rate, and turbulent eddy dissipation rate, are shown for a storm penetration during Run 2 on 11 June. The 2D-C samples 5 $\ell s^{-1}$.*

The data from Run 3, a subsequent pass through the same storm about 12 minutes later, from southwest-to-northeast, are shown in Figure 10. There is now a somewhat weaker, less-organized updraft with lower peak vertical wind, lower cloud water concentration, and somewhat higher precipitation particle concentration and turbulence within the updraft, although peak values of both precipitation and turbulence are concentrated outside of the updraft. It must be noted that it is not clear that the aircraft passed through the center of the updraft on either run, and so the differences in character between the two passes involve spatial as well as temporal variation.

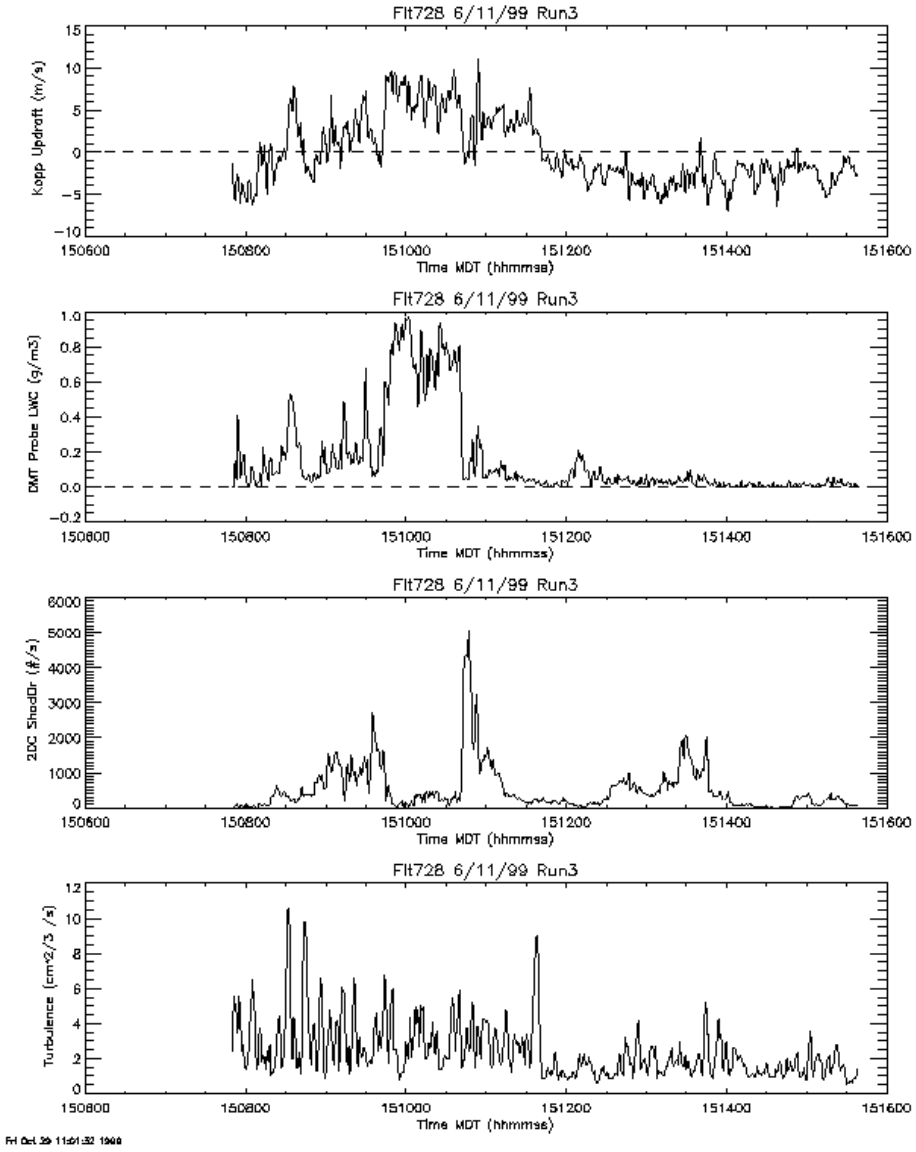


*Figure 10: The same parameters are shown for the next pass through the same storm as in Figure 9.*

Additional information is collected in 4 appendices. Appendix A summarizes the T-28 instrumentation. Appendix B summarizes the parameters routinely computed based on instrumentation readings. Appendix C summarizes the data reduction algorithm. Appendix D contains maps of the T-28 track during each mission. Colored stems pointing perpendicularly from the track have lengths in proportion to the magnitude of turbulence computed using the algorithm of Sand *et al.* (1976) (red), and in proportion to the precipitation particle concentration detected by the PMS OAP-2DC probe (green). It can be seen that precipitation particle concentration and turbulent energy dissipation rate are often roughly correlated, but that there are many instances of high magnitudes of one of these parameters accompanied by lower magnitudes of the other.

This preliminary data survey suggests that the data obtained during this program are physically consistent with the expected properties of convective storms in this region. More sophisticated analyses are warranted to focus on the program objectives of a detailed characterization of turbulence in and around convective clouds, and testing of techniques for using Doppler airborne weather radars to quantitatively characterize this turbulence.

## Acknowledgements

It is a pleasure to acknowledge the generous assistance and cooperation of our colleagues from the NASA Langley Research Center, from Allied Signal/Honeywell and Rockwell-Collins, from the National Center for Atmospheric Research Research Applications group, and from the CSU-CHILL research radar facility. The Jet Center at Fort Collins –Loveland Regional Airport provided excellent facilities and flight support. Funding for the T-28 deployment came through the Aviation Safety Program at NASA Langley.

## References

Cornman, L.B., C.S. Morse, and G. Cunning, 1993: Estimation of atmospheric turbulence severity from in-situ aircraft measurements. Preprints, *International Conference on Aviation Weather Systems*, August 2-6, 1993, Vienna, Virginia. American Meteorological Society, Boston, 152-156.

Gardiner, B.A., and J. Hallett, 1986: Degradation of in-cloud Forward Scattering Spectrometer Probe measurements in the presence of ice particles. *J. Atmos. Ocean. Tech.,* **2**, 171-180.

Knight, C.A., and P. Squires, (eds.), 1982: *Hailstorms of the Central High Plains. Vol. I: The National Hail Research Experiment.* Colorado Assoc. Univ. Press, Boulder, CO. 282 pp.

Kopp, F. J., 1985: Deduction of vertical motion in the atmosphere from aircraft measurements. *J. Atmos. Ocean Tech.,* **2**, 684-688.

MacCready, P.B., Jr., 1962: Turbulence measurements by sailplane. *J. Geophys. Res*., **67**, 1041-1050.

Sand, W.R., J.L. Halvorson and T.G. Kyle, 1976: Turbulence measurements inside thunderstorms used to determine diffusion characteristics for cloud. *Proc. 2nd World Meteorological Organization Conference on Weather Modification,* Boulder, CO, 539-545.

# Appendix A – Instrumentation Table

| VARIABLE | INSTRUMENT | RANGE | ACCURACY | RESOLUTION (as recorded) | NOTES |
|---|---|---|---|---|---|
| Static Pressure | Rosemount 1301-A-4B | 0-15 psi (0-103 kPa) | ±0.015 psi (±0.1kPa) | 0.0002 psi (0.002 kPa) | |
| | Rosemount 1301-A-4B | 5-15 psi (35-103 kPa) | ±0.015 psi (±0.1kPa) | 0.0002 psi (0.002 kPa) | |
| Total Temperature | Rosemount 102AU2AP | -30 to +30°C | ±0.5°C | 0.001°C | • Platinum wire<br>• 2 s time constant |
| | NCAR Reverse Flow | -30 to +30°C | ±0.5°C | 0.001°C | • Platinum RTD element<br>• Several seconds time constant |
| Cloud Water and Cloud Droplets | DMT Liquid Water Concentration | 0 - 4 g/m$^3$ | ±20% | 0.0001 g/m$^3$ | • Sampling rate 4 l/km |
| | Particle Measuring Systems, Inc. Forward Scattering Spectrometer Probe | Size 1 < 67 µm Concentration<br>0 - 2000 droplets/cm$^3$ | ±1 size channel in size and ±1% in concentration at ~50/cm$^3$ | 1 size channel | • 15 discrete size channels spread over an adjustable range<br>• Sampling rate 300 cm$^3$/km<br>• Accuracy of computed liquid water concentration ~±50%. Depends on processing. |
| Precipitation Particle Sizes And Concentrations | Particle Measuring Systems, Inc. 2D Cloud Probe | Size 25 - 800 µm | ±25 µm | 25 µm | • Computed ice and water mass concentration can vary ±50% with processing technique<br>• Sampling rate: 0.05 m$^3$/km; DAS can accept ~250 particles/s (2500/km) |
| | Hail Spectrometer | Size 4.5 mm - 4.5 cm Concentration 0 - 100/m$^3$ | ±1 size class | 1 size class | • 14 size classes, and images<br>• Sampling rate 100 m$^3$/km |
| Aircraft Motion | Humphrey SA09-D0101-1 Vertically Stabilized Accelerometer | ±2 g's<br>pitch –50° to 50°<br>roll –50° to +50° | 0.004 g's<br>0.2°<br>0.2° | 0.00006 g<br>0.002°<br>0.002° | |
| | Rosemount 1301-D-1b Dynamic Pressure | –3 to +3 psi (–20 to +20 kPa) | ±0.1% | 0.0001 psi (0.0006 kPa) | |
| | Rosemount 1221-F-2A Dynamic Pressure | –2.5 to +2.5 psi (–18 to +18 kPa) | ±0.1% | 0.0001 psi (0.0006 kPa) | |
| | Giannini 45218YE Manifold Pressure | 0 to 50 in Hg | ±2% | 0.008 Hg (0.03 kPa) | • Used in backup vertical velocity calculation |
| | Crossbow Non-Stabilized 3-Axis Accelerometer | ±4 g in all 3 directions | ±0.2% | 3.05 x ($10^{-4}$ g's) | |
| Aircraft Location | Trimble TNL2000 GPS | (global) | 30 m | 18 m | |
| Electric Field | NMIMT Model E-100 DC Electric Field Meter | top/bot ± 650 kV<br>wingtips ±3200 kV<br>5th and 6th ±340 m | | (coarse resolution)<br>0.01 kV/m | |

NOTE: Many of these instruments do not behave as ideal instruments. The use of one measure of accuracy over the entire range of measurement is, in many cases, questionable. An accuracy representative of the most useful part of the range is given here. Revised 11/99

# Appendix B – Data Dictionary

| Tag | Variable | Remarks |
|---|---|---|
| | | |
| 100 | **Time** | The T-28 data system is set to MDT, and recorded in a 24-hour format. For this project, it has been converted to UT in post-processing. It is set daily within a second of WWV, but suffers loss of a second or two each time system is booted. |
| | | |
| 101 | **Dynamic Pressure 1** | |
| | | |
| 102 | **Dynamic Pressure 2** | Both dynamic pressures are read from the same pitot tube line (with the inlet out on the right wing) using two different but nearly identical sensors. [hPa] |
| | | |
| 103 | **Static Pressure 1** | |
| | | |
| 104 | **Static Pressure 2** | Both static pressures are read from the same static pressure line (inlet on the rear fuselage) using two different but nearly identical sensors. [hPa] |
| | | |
| 105 | **Rate of Climb** | The instantaneous rate of change of aircraft altitude, read from a standard aircraft variometer. The recorded data are unfiltered and much noisier than the damped cockpit display. This instrument was removed after Flt. 725. [m $s^{-1}$] |
| | | |
| 106 | **Rosemount Temperature** | This is static temperature computed from the reading of a standard, deiced, Rosemount aircraft total air temperature probe. It commonly suffers from wetting and reads low in clouds. [°C] |
| | | |
| 107 | **Reverse Flow Temperature** | This is static temperature computed from the reading of a platinum resistance element placed inside a custom-design "reverse-flow" housing. It normally does not get wet in cold clouds or in regions of high precipitation water concentration. Apparently, ice may sometimes build up to such an extent on the housing that temperature readings are affected even though the sensor is not wetted. Its response to changes in angle of attack is greater than that of the Rosemount probe. [°C] |
| | | |
| 108 | **Manifold Pressure** | Pressure inside the engine manifold (an indicator of power being developed by the engine) is recorded from a standard aircraft engine presssure sensor. [inches of mercury] |
| | | |
| 109 | **Acceleration** | Vertical acceleration is determined by a Humphrey gyro-stabilized accelerometer. [g's] |
| | | |
| 110 | **Pitch** | The accelerometer also gives angle of the fuselage relative to horizontal (positive for nose up). [deg] |
| | | |

| | | |
|---|---|---|
| 111 | **Roll** | The accelerometer also gives angle of the wings relative to horizontal. Angle is positive for a left bank (left wing down). [deg] |
| | | |
| 113 | **VOR** | The VOR gives the direction to the VORTAC (a radio direction-finding beacon used by aircraft) to which it is tuned. [deg] |
| | | |
| 114 | **DME1** | This is distance to the VORTAC to which the DME is tuned. [n mi] |
| | | |
| 116 | **Voltage Regulator** | Voltage of power source for some instruments. [volts] |
| | | |
| 117 | **Heading** | Indicates direction (from magnetic north) towards which the aircraft is heading. [deg] |
| 118 | **NCAR True Airspeed** | Airspeed computed by an analog circuit; can be used to clock PMS OAP-2D probes. Less accurate than "Calculated TAS", Tag 211 |
| | | |
| 119 | **PMS End Element 1** | Voltage readings of PMS OAP-2D probe end diodes. Used to monitor for fogging and icing of probe. |
| | | |
| 120 | **PMS End Element 2** | |
| | | |
| 121 | **Interior Temperature** | Temperature inside the data acquisition system computer in the baggage bay. [°C] |
| | | |
| 124 | **Heater Current** | Total current consumed by de-icing circuits (A). |
| | | |
| 130 | **Event Bits** | Bits corresponding to various events recognized by the data system, including an indication that the system is running, that the in-cloud switch is activated by the pilot (when visually entering cloud), that the foil impactor is running, and that the cockpit voice recorder is activated. |
| | | |
| 131 | **GPS Warning Codes** | Bits corresponding to various status messages from the GPS system. |
| | | |
| 140 | **FSSP size counts** | This tag contains information concerning the number of counts in each of the 15 available FSSP size channels. [number per channel per second] |
| | | |
| 141 | **FSSP total counts** | The total number of droplets counted by the FSSP during a second. |
| | | |
| 142 | **FSSP average diameter** | The arithmetic average diameter of all droplets recorded during a second. [µm] |
| | | |
| 143 | **FSSP concentration** | The number of droplets computed from FSSP counts divided by the volume sampled in 1 s. A rudimentary correction for probe activity is made. [# $cm^{-3}$] |
| | | |

| | | |
|---|---|---|
| 144 | **FSSP Water** | The liquid water concentration computed from the FSSP data for a second. [g $m^{-3}$] |
| | | |
| 145 | **FSSP Activity** | The fraction of time the FSSP is active during the current second. |
| | | |
| 147 | **PMS 2DC Shadow Or Count** | The number of times the 2D probe was triggered out of its wait state by the passage of a new particle. [# $s^{-1}$] |
| | | |
| 148 | **FSSP Equivalent Diameter** | $\sum_{i=1}^{15}\left[\frac{n_i \cdot d_i^3}{n_i \cdot d_i^2}\right]$ |
| | | |
| 149 | **Variance in FSSP Equivalent Diameter** | Variance around the equivalent diameter, computed as $\frac{\sum_{i=1}^{15} n_i \cdot d_i^2 \cdot \left(d_i - d_{eqv}\right)^2}{d_{eqv}^2 \cdot \left(\sum_{i=1}^{15} d_i\right)^2}$ |
| | | |
| 150 | **Hail size counts** | This tag contains information on the number of particles in each of the 14 hail spectrometer size channels. [number per channel per second] |
| | | |
| 151 | **Slow Particle** | The number of particles rejected because they passed through the hail spectrometer too slowly (indicating they were probably water or ice shed from the probe structure rather than airborne hydrometeors). [number per second] |
| | | |
| 152 | **Hail total counts of (150)** | Total number of particles accepted by the hail spectrometer. [number per second] |
| | | |
| 153 | **Hail average diameter** | The average diameter of all particles accepted by the hail spectrometer in the last second. [cm] |
| | | |
| 154 | **Hail concentration** | The computed concentration corresponding to all particles accepted by the hail spectrometer in the last second. [number per cubic meter] |
| | | |
| 155 | **Hail Water** | The mass concentration computed from the observed particle spectrum assuming spherical particles and a bulk particle density of 0.9 grams per cubic centimeter. [grams per cubic meter] |
| | | |
| 160 | **Top Field Mill** | The electric field indicated by the low sensitivity channel on the field mill mounted in the aircraft canopy looking up. Field mill data are recorded at 20 Hz. [kV $m^{-1}$] |
| | | |

| | | |
|---|---|---|
| 161 | **Bottom Field Mill** | The electric field indicated by the low sensitivity channel on the field mill located in the baggage bay door looking down. [kV $m^{-1}$] |
| | | |
| 162 | **Left Field Mill** | The electric field indicated by the low sensitivity channel on the field mill mounted in the left wing tip facing outward. [kV $m^{-1}$] |
| | | |
| 163 | **Right Field Mill** | The electric field indicated by the low sensitivity channel on the field mill mounted in the right wing tip facing outward. [kV $m^{-1}$] |
| | | |
| 168 | **Fifth Field Mill** | The electric field indicated by the low sensitivity channel on the fifth field mill, located forward in one of the hail spectrometer pylons under the left wing. [kV $m^{-1}$] |
| 169 | **Sixth Field Mill** | The electric field indicated by the low sensitivity channel on the $6^{th}$ field mill, located aft in the hail spectrometer pylon under the left wing (kV $m^{-1}$) |
| | | |
| 172 | **Latitude** | Computed internally in the GPS receiver. [deg] |
| | | |
| 173 | **Longitude** | Also computed internally in the GPS receiver. [deg] |
| | | |
| 174 | **Groundspeed** | Computed internally in the GPS receiver (by differentiating the position data with respect to time). [m/s] |
| | | |
| 175 | **Ground Track Angle** | The direction towards which the aircraft is moving relative to the ground, with respect to magnetic north. [deg] |
| | | |
| 176 | **Magnetic Deviation** | The difference between magnetic north and true north as indicated automatically by the GPS receiver based on the current position. [deg] |
| | | |
| 177 | **Time Since Solution** | The time since the GPS was last able to compute an accurate position solution based on a sufficient number of satellites. The GPS updates position based on dead reckoning if it does not have a sufficient number of satellites in view. [s] |
| | | |
| 178 | **GPS Altitude** | Geometric aircraft altitude. [m MSL]] |
| | | |
| 190 | **FSSP Gated Strobes** | Number of accepted droplet counts. [# $s^{-1}$] |
| | | |
| 191 | **FSSP Total Strobes** | Total number of droplet counts. [# $s^{-1}$] |
| | | |
| 192 | **FSSP Reference Voltage** | Reference voltage for FSSP opto-electronics. |
| | | |

| | | |
|---|---|---|
| 200 | **Date** | As indicated by the data acquisition system computer clock. [yymmdd] |
| | | |
| 201 | **Month** | mm [integer number] |
| | | |
| 202 | **Day** | dd [integer number] |
| | | |
| 203 | **Year** | yy [integer number] |
| | | |
| 204 | **Flight** | A serial number assigned to each T-28 flight beginning with the "first" research flight. (Flight #1 occurred in 1972.) |
| | | |
| 205 | **Altitude** | The altitude in a standard atmosphere corresponding to the recorded static pressure. [m] |
| | | |
| 206 | $\theta_e$ | The equivalent potential temperature corresponding to the recorded temperature and assuming saturation with respect to liquid water (should be valid in-cloud). [K] |
| | | |
| 207 | **Saturation Mixing Ratio** | The mixing ratio of water vapor corresponding to saturation with respect to liquid water at the recorded temperature. [g $kg^{-1}$] |
| | | |
| 208 | **Point dz/dt** | The rate of change of altitude of the aircraft computed by differentiating the pressure altitude with respect to time. |
| | | |
| 209 | **Indicated Air Speed** | What the airspeed would be if the aircraft were flying at sea level and indicating the observed dynamic presure. [m $s^{-1}$] |
| | | |
| 210 | **Updraft (uncorrected)** | The estimated upward speed of the air relative to the ground computed from changes in the aircraft altitude and other factors, but not corrected for horizontal aircraft acceleration. [m $s^{-1}$] |
| | | |
| 211 | **Calculated TAS** | The true speed of the aircraft relative to the air computed from the observed dynamic and static pressures, and temperature. [m $s^{-1}$] |
| | | |
| 212 | **Updraft Correction Factor** | A correction to tag 210, the simple (uncorrected) updraft calculation, that accounts for horizontal accelerations of the aircraft. [m $s^{-1}$] |
| | | |
| 213 | **Cooper Updraft** | The sum of the uncorrected updraft (210) and the correction factor (211). [m $s^{-1}$] |
| | | |
| 214 | **Kopp Updraft** | A more reliable updraft estimate calculated using methods discussed in Kopp, 1985. In most situations, it yields a less noisy and more physically plausible updraft result for the T-28 than the Cooper method. [m $s^{-1}$] |

| | | |
|---|---|---|
| | | |
| 216 | **Turbulence** | The turbulent energy dissipation rate estimated from the spectrum of observed fluctuations in true airspeed following a method developed by MacCready. [$cm^{2/3}$ $s^{-1}$] |
| | | |
| 217 | **Air Density** | Computed from the recorded temperature and static pressure. [$kg\ m^{-3}$] |
| | | |
| 219 | **FSSP Mixing Ratio** | The mixing ratio of cloud water per unit mass of dry air calculated from the FSSP water concentration. [$g\ kg^{-1}$] |
| | | |
| 220 | **Hail Mixing Ratio** | The mixing ratio of hail mass per unit mass of dry air based on the computed hail water and air density. [$g\ kg^{-1}$] |
| | | |
| 244 | **FSSP equivalent J-W Liquid Water** | An estimate of the liquid water concentration a J-W probe should record, based on the observed FSSP droplet spectrum and the assumption that a J-W probe responds incompletely to droplets larger than 30 $\mu$m diameter. [$g\ m^{-3}$] |
| | | |
| 260 | **Ambient Vert Electric Field** | The component of the ambient electric field that is vertical in the aircraft frame of reference. Positive means a positive test charge would drift upward relative to the aircraft in the field. [$kV\ m^{-1}$] |
| | | |
| 261 | **Vert Electric Field due to aircraft charge** | The field due to charge on the aircraft, computed by summing the readings of the top and bottom mill and normalizing based on self-charging tests. Positive means a positive test charge would be repelled away from the aircraft due to its charge. [$kV\ m^{-1}$] |
| | | |
| 262 | **Ambient Hor Electric Field** | The ambient field oriented perpendicular to the aircraft along the wings, positive meaning a positive test charge would drift to the right in the field. [$kV\ m^{-1}$] |
| | | |
| 263 | **Hor Electric Field due to aircraft charge** | The field due to charge on the aircraft, computed by summing the wingtip mill readings and normalizing. Positive means a positive charge would be repelled away from the aircraft due to its charge. [$kV\ m^{-1}$] |
| | | |
| 264 | **Ambient Vert Field (roll cor)** | The component of the ambient field that is truly vertical with respect to earth coordinates. [$kV\ m^{-1}$] |
| | | |
| 265 | **Ambient Hor Field (roll cor)** | The component of the ambient field perpendicular to the aircraft path and truly horizontal with respect to earth coordinates. [$kV\ m^{-1}$] |
| 266 | **Ex** | X-component of ambient horizontal electric field, based on Mo et al (1999). Positive means a positive test charge would drift in the direction of the aircraft under the influence of the field. [$kV\ m^{-1}$] |

| | | |
|---|---|---|
| 267 | **Ey** | Y-component of ambient horizontal electric field, based on Mo et al (1999). Positive means a positive test charge would drift to the right of the direction of the aircraft under the influence of the field. [kV $m^{-1}$] |
| | | |
| 268 | **Ez** | Z-component of ambient electric filed, based on Mo et al (1999). Positive means a positive test charge would drift upward under the influence of the field. [kV $m^{-1}$] |
| | | |
| 272 | **Latitude (deg)** | GPS coordinates broken into separate degree and minute components. |
| | | |
| 273 | **Latitude (min)** | GPS coordinates broken into separate degree and minute components. |
| | | |
| 274 | **Longitude (deg)** | GPS coordinates broken into separate degree and minute components. |
| | | |
| 275 | **Longitude (min)** | GPS coordinates broken into separate degree and minute components. |
| | | |
| 276 | **Ground Track Angle (True N)** | The direction of motion relative to the ground with respect to true north, derived from the GPS ground track angle with respect to magnetic north. [deg] |
| | | |
| 290 | **X-acceleration** | Acceleration in the direction of aircraft motion. Acceleration backward (deceleration) yields a positive value. [g's] |
| | | |
| 291 | **Y-acceleration** | Acceleration perpendicular to the direction of aircraft motion, along the direction of the wings. Acceleration toward the left yields a positive value. [g's] |
| | | |
| 292 | **Z-acceleration** | Vertical acceleration. Upward acceleration produces a positive value. [g's] |

## APPENDIX C: DATA REDUCTION FORMULAE TABLE

Reduced Data Items Computed for Turbulence Project
Loveland, CO June, 1999 (see footnote 1)

| *Tag #* | *Description* | *Output* | *# Values* *Units* | *Method of Computation* | *Last Mod (if this project)* | |
|---|---|---|---|---|---|---|
| | | | | | | |
| 101 | Dynamic Pressure #1 | (20 Hz) | 1 mb | 6.30452E–3 * Raw – 0.0489 | | |
| 102 | Dynamic Pressure #2 | (20 Hz) | 1 mb | 5.28371E–3 * Raw – 1.5768 | | |
| 103 | Static Pressure #1 | (20 Hz) | 1 mb | 1.5791E–2 * Raw + 530.37 | | |
| 104 | Static Pressure #2 | (20 Hz) | 1 mb | 1.0917E–2 * Raw + 691.92 | | |
| 105 | Rate of Climb | (20 Hz) | 1 m/s | 5.625E–4 * Raw, for Raw > = 0 | | |
| | | | | 5.287E–4 * Raw, for Raw < 0 | | |
| 106 | Rosemount Temp | | 1 deg C | mach2 = 5*((l +dyn_pr/stat_pr)**(2/7)-l) | | |
| | | | | divisor = 1 + 0.195 * mach2 | | |
| | | | | temp = (1.83105E-3 * Raw + 243.16)/divisor-273.16 | | |
| 107 | Reverse Flow Temp | | 1 deg C | divisor = 1 + 0.1594 * mach2 | | |
| | | | | temp = (3.02109E-3 * Raw + 222.06)/divisor-273.16 | | |
| 108 | Manifold Pressure | | 1 " Hg | 3.1098E-3 * Raw + 0.159275 | | |
| 109 | Acceleration | (20 Hz) | 1 g's | 6.25E–5 * Raw [prior to 7/14/94] | | |
| | | | | 6.25E–5 * Raw + 1.0 [after 7/14/94] | | |
| 110 | Pitch | (20 Hz) | 1 deg | –3.05175E–3 * Raw + 50 | | |
| 111 | Roll | (20 Hz) | 1 deg | 3.05175E–3 * Raw – 50 | | |
| 113 | VOR | | 1 deg | 1.117534E–2 * Raw – 1.155475 | | |
| 114 | DME #1 | | 1 naut mi | 3.03269E–3 * Raw – 0.24536 | | |
| 116 | Voltage Regulator | | 1 volts | 1.5258789E–4 * Raw | | |
| 117 | Heading | (20 Hz) | 1 deg | interpolation from lookup table | | |
| 118 | NCAR true air speed | | 1 m/s | 3.96744E–3 * Raw | | |
| 121 | Interior Temp (computer) | | 1 deg C | 3.05175E–2 * Raw | | |
| 124 | Heater current | | 1 amp | 3.05175E–3 * Raw | | |
| 128 | Discharging (Forward) | | 1 | 1.52588E–4 * Raw | | |
| 129 | Discharging (Aft) | | 1 | –1.52588E–4 * Raw | | |
| 130 | Event Code bits | | 1 flags | bit 0 = 1 --> system running | | |
| | | | | bit 1 = 0 -- > in cloud | | |

| | | | | | | | |
|---|---|---|---|---|---|---|---|
| | | | | | bit 2 = 0 -- > foil on | | |
| 131 | GPS warning codes | | 1 | flags | 11 bit codes | | |
| 140 | FSSP counts | | 15 | number | Raw | | |
| 141 | FSSP total counts | | 1 | number | Sum of tag 140s (tot_count) | | |
| 142 | FSSP ave diameter | | 1 | μm | sum of diams / (tot_count) | | *2 |
| 143 | FSSP concentration | | | $cm^3$ | vol = 0.22275 * tas (volume sampling rate ($m^3$/s))<br>(.22275 $mm^2$ = sampling area) | | *2 |
| | | | | | denom = 1 – .55 * activ / 100 (adjustment for probe activity) | | |
| | | | 1 | $\#/cm^3$ | conc = tot_count /vol / denom | | |
| | FSSP total mass | | | g | mass = sum of counts * volumes | | *2 |
| 144 | FSSP water | | 1 | $g/m^3$ | water = mass / vol / denom * 1.E6 | | |
| 145 | Probe Activity | | 1 | % | Raw / 10 | | |
| 148 | FSSP equivalent diameter | | 1 | μm | Ratio of sum of diam **3 to sum of diam **2 | | *2 |
| 149 | FSSP equivalent diameter variance | | 1 | μm | Consult listing or Appendix B (Data Dictionary) | | *2 |
| 150 | Hail counts | | 14 | number | Raw | | |
| 151 | Hail slow particle count | | 1 | number | Channel 15 | | |
| 152 | Hail total counts | | 1 | number | Sum of tag 150s (tot_counts) | | |
| 153 | Hail ave diameter | | 1 | cm | sum of diams / tot_counts | | |
| 154 | Hail concentration | | 1 | $\#/m^3$ | conc = tot_counts / (0. 1 * tas)<br>0.1 $m^2$ = sampling area<br>(0.1 * tas) = volume sampling rate ($m^3$/s) | | |
| | Hail total mass | | | g | mass = $\Sigma_i$ $count_i$ * $volume_i$ * 0.9 (0.9 $g/cm^3$ = hail density) | | |
| 155 | Hail water | | 1 | $g/m^3$ | water = mass / (0. 1 * tas) | | |
| 160 | Top field mill, low res | (20 Hz) | 1 | kV/m | –2.1117E-2 * Raw + 0.094 | | |
| 161 | Bottom field mill, low res | (20 Hz) | 1 | kV/m | –2.091E-2 * Raw + 0.181 | | |
| 162 | Left field mill, low res | (20 Hz) | 1 | kV/m | –9.6722E-2 * Raw – 0.975 | | |
| 163 | Right field mill, low res | (20 Hz) | 1 | kV/m | –9.7641E-2 * Raw – 2.076 | | |
| 168 | Fifth field mill, low res | (20 Hz) | 1 | kV/m | –9.9154E-2 * Raw + 6.49 | | |
| 169 | Sixth field mill, low res | (20 Hz) | 1 | kV/m | 1.5258789E-4 * Raw (voltage only, no calibration yet) | June 1999 | |
| 172 | GPS latitude | | 1 | deg | degree + (minute + hundredths/100)/60 | | |
| 173 | GPS longitude | | 1 | deg | degree + (minute + hundredths/100)/60 | | |
| 174 | GPS groundspeed | | 1 | m/s | 1852 / 36000 * Raw | | |

| | | | | | | | |
|---|---|---|---|---|---|---|---|
| 175 | GPS grnd track angle (mag N) | | 1 | deg | Raw / 10 | | |
| 176 | GPS magnetic deviation | | 1 | deg | Raw / 10 (Raw is 32-bits, not 16) | | |
| 177 | GPS time since solution | | 1 | s | Raw /10 | | |
| 178 | GPS altitude | | 1 | m | Raw / 10 / .3048 (Raw is 32-bits, not 16) | | |
| 185 | GPS ROC | | 1 | m/s | 10ths of ft/min to m/s | | |
| 186 | DMT LW | | | | p = 20 * Raw * 1.5258789E-4 (p = Power)<br>tlfm = (twk + tk)/2 (twk = Wire Temp; tk = Air Temp) | | |
| | Thermal Conductivity | | | | cnd = 5.8E-5 * (398 / (125 + tflm)) * (tflm/273)^1.5<br>cndw = 5.8E–5 * (398/(125 + twk))* (twk/273)^ 1.5 | | |
| | Viscosity | | | | visc = 1.718E–4 * (393/(120 + tflm)) * (tflm/273) ^1.5<br>vscw = 1.718E–4 * (393/(120 + twk)) * (twk/273)^1.5 | | |
| | Density | | | | dens = pres / (2870.5 * tflm) (pres = Pressure) | | |
| | | | | | fct = $\pi$ * l * cnd * (twk – tk) (l = Wire Length) | | |
| | Reynold's Number | | | | re = 100 * dens * tas * d/visc (tas = True Air Speed) | | |
| | Prandtl Numbers | | | | prf = 0.24 * visc/cnd<br>prw = 0.24 * vscw/cndw | | |
| | Dry Air Loss | | | | dryp = 0.26 * re ^ 0.6 * prf ^ 0.37 * (prf/prw) ^ 0.25 * fct/0.239<br>fact = 1.238E6 * 0.239/(tas * 100 * (597.3 + 373.16 – tk)) | | |
| | LWC | | 1 | $g/m^3$ | lwc = (p–dryp) * fact | | |
| 190 | FSSP gated strobes | | 1 | number | Raw | | |
| 191 | FSSP total strobes (div by 10) | | 1 | number | Raw | | |
| 192 | FSSP reference voltage | | 1 | volts | Raw / 25.5 | | |
| 200 | Date | | 1 | yymmdd | | | |
| 201 | Month | | 1 | number | | | |
| 202 | Day | | 1 | number | | | |
| 203 | Year | | 1 | 2-dig | | | |
| 204 | Flight number | | 1 | number | | | |
| 205 | Altitude | | 1 | m | 4.43077E4 * (1 –(stat_pr/l013.3027)**.190284) (stat_pr = Static Pressure) | | |
| 206 | $\theta_e$ | | 1 | K | | | |
| | Saturation Vapor Pressure | | | mb | svp = 6.1078 * exp(17.26939 * rft/(tempk–35.86))<br>(tempk = RFT in K) | | |
| | Saturation Mixing Ratio | | | kg/kg | smr = svp / (stat_pr – svp) * 0.622 | | |
| | | | | K | ts = tempk * (1000/stat_pr) **0.286 | | |
| | $\theta_e$ | | | K | thetae = ts * exp(597.3*smr)/(0.24*tempk)) | | |

| | | | | | | | |
|---|---|---|---|---|---|---|---|
| 207 | Saturation mixing ratio | | 1 | kg/kg | smr from above | | |
| 208 | Point dz/dt | | 1 | m/s | (alt - prev_alt (2 secs previous)) / 2 | | |
| 209 | Indicated airspeed | | 1 | m/s | c = 1 + dyn_pr / 1013.3027 | | |
| | | | | | ias = sqrt(5.79E5*(c**(2/7)–l)) | | |
| 210 | Updraft (uncorrected) | | 1 | m/s | ul = change in alt ((i + l) – (i–1))/2 | | |
| | | | | | u2 = (27 - man_pr) * 92 | | |
| | | | | | u3 = (1.94254 * ias - 140) * 17.7 | | |
| | | | | | updr = ul + (u2 + u3) * 0.00508 | | |
| 211 | Calculated TAS | | 1 | m/s | sqrt(rftuc * mach2 * 401.856/divisor) | | |
| 212 | Updraft correction factor | | 1 | m/s | $gps\_gs_1$ * ($gps\_gs_0$ – $gps\_gs_2$)/2/9.775 (gps_gs = GPS Groundspeed) 0) current 1) 1 sec previous 2) 2 secs previous | | |
| 213 | Cooper Updraft | | 1 | m/s | updraft + updraft correction factor | | |
| 214 | Kopp Updraft | | 1 | m/s | dens = 0.34838 * stat_pr /tempk | | |
| | | | | | ang = pitch * 0.0174533 | | |
| | | | | | Kopp = ul + 62.12 * accel * 9.775/(dens * calc_tas) | | |
| | | | | | –(0.02028+ang) * calc_tas | | |
| 216 | Turbulence | | 1 | $cm^{2/3}/s$ | Weighted sum of calculated TAS power spectrum | | |
| | | | | | Static and dynamic pressure values, along with RFTs, are fed into a fast Fourier transform routine. Consult program listing. | | |
| 217 | Air density | | 1 | $kg/m^3$ | 0.34838 * stat_pr / tempk | | |
| 218 | JW mixing ratio | | 1 | g/kg | jw_water / density | | |
| 219 | FSSP mixing ratio | | 1 | g/kg | FSSP_water / density | | |
| 220 | Hail mixing ratio | | 1 | g/kg | hail_water / density | | |
| 221 | RFT uncorrected | | 1 | deg C | Reverse flow temp without divisor term | | |
| 244 | JW equiv water | | 1 | $g/m^3$ | mass = sum of counts * volumes, where diams > 30 | | |
| | | | | | microns are treated as equal to 30 | | |
| | | | | | water = mass/vol/denom * 1.E6 | | |
| 260 | Ambient vert EF | | 1 | kV/m | (tfm - 2 * bfm) / 11.2 | | |
| 261 | Plane vert EF | | 1 | kV/m | (tfm + 2 * bfm) / 11.2 | | |
| 262 | Ambient lateral EF | | 1 | kV/m | (rfm – lfm) / 44.8 | | |
| 263 | Plane lateral EF | | 1 | kV/m | (rfm + lfm) / 32.48 | | |
| 264 | Ambient vert EF (with roll) | | 1 | kV/m | cosr = cos(roll_rad) | | |
| | | | | | sinr = sin(roll_rad) | | |

| | | | | | | | |
|---|---|---|---|---|---|---|---|
| | | | | | t264 = t260 * cosr + t262 * sinr | | |
| 265 | Ambient lat EF (with roll) | | 1 | kV/m | t265 = -t260 * sinr + t262 * cosr | | |
| 266 | $E_{xq}$ (Mo *et al.* 1999) | | 1 | kV/m | 0.0357 * lfm + 0.0496 * rfm + 0.0528 * fm5 | | |
| 267 | $E_y$ (Mo *et al.* 1999) | | 1 | kV/m | –(0.0231 * lfm - 0.0230 * rfm + 0.0031 * fm5) (new method for $E_y$) | | |
| 268 | $E_z$ (Mo *et al.* 1999) | | 1 | kV/m | 0.0843 * lfm + 0.0229 * rfm – 0.1735 * fm5 (new method for $E_z$) | | |
| 269 | $E_y$ (267) - $E_y$ (262) | | 1 | kV/m | t267 - t262 (Difference between old and new methods) | | |
| 270 | $E_z$ (268) - $E_z$ (260) | | 1 | kV/m | t268 - t260 (Difference between old and new methods) | | |
| 272 | GPS deg lat | | 1 | deg | integer portion of tag 172 (t172) | | |
| 273 | GPS min lat | | 1 | min | fractional part of t172 * 60 | | |
| 274 | GPS deg long | | 1 | deg | integer portion of tag 173 (t173) | | |
| 275 | GPS min long | | 1 | min | fractional part of t173 * 60 | | |
| 276 | GPS true bearing | | 1 | deg | mod(t175 + t176 + 360,360) | | |
| 290 | Accelerometer (x) | (20 Hz) | 1 | g's | (Raw * 1.5258789E-4 – 2.511) / 0.492 | | |
| 291 | Accelerometer (y) | (20 Hz) | 1 | g's | (Raw * 1.5258789E-4 – 2.49) / 0.5 | | |
| 292 | Accelerometer (z) | (20 Hz) | 1 | g's | (Raw * 1.5258789E-4 – 2.513) / 0.503 | | |

*1 In some cases the equation variables are averages. Consult the listing for exact details. All quantities are recorded at 1 Hz unless otherwise noted.

*2 Calibration of the FSSP (via bead test) led to new channel assignments in file FSSP.CHN for 1999.

# Appendix D – Flight Tracks

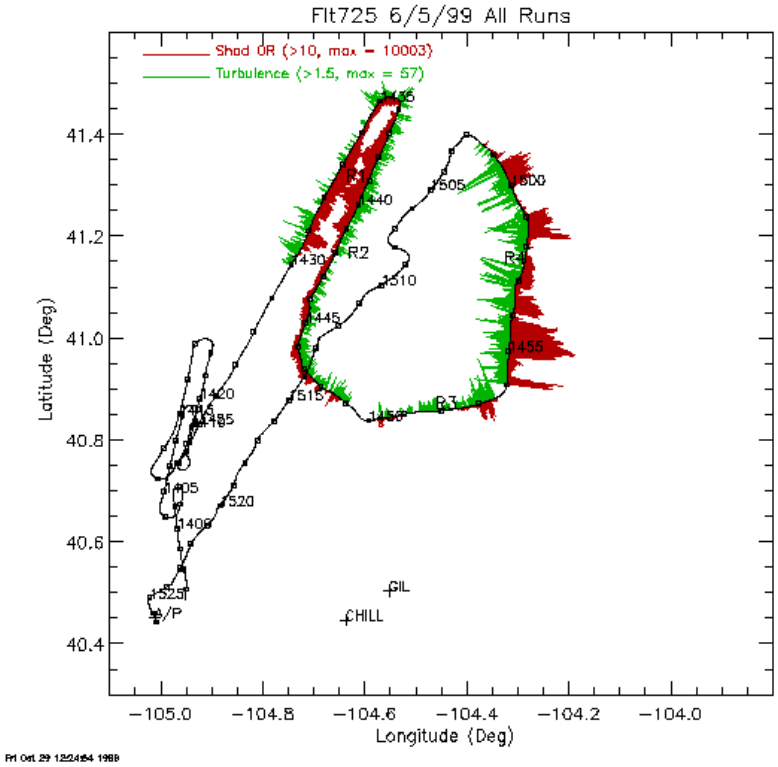


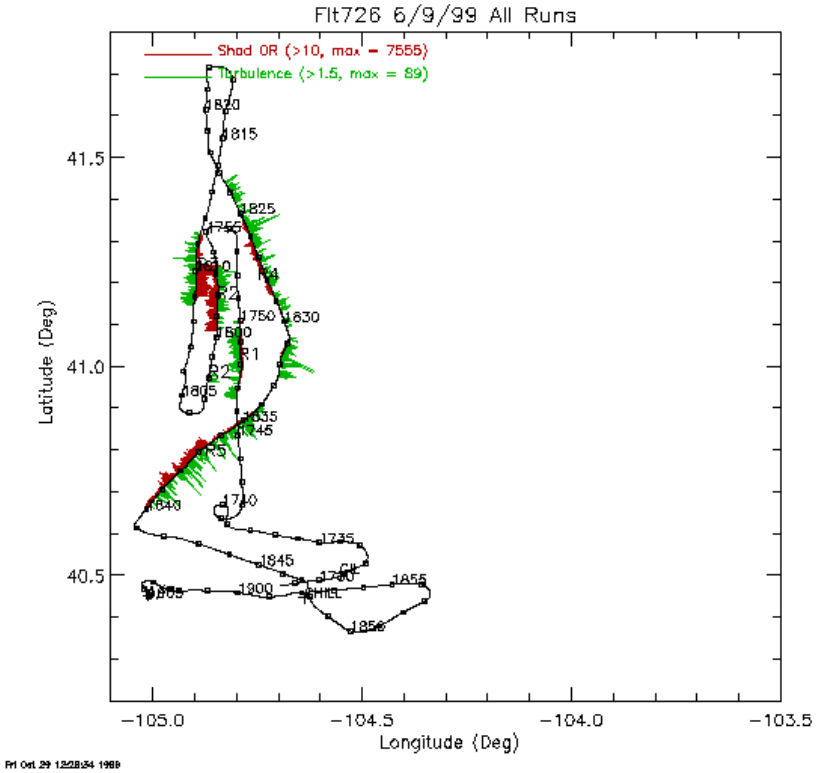

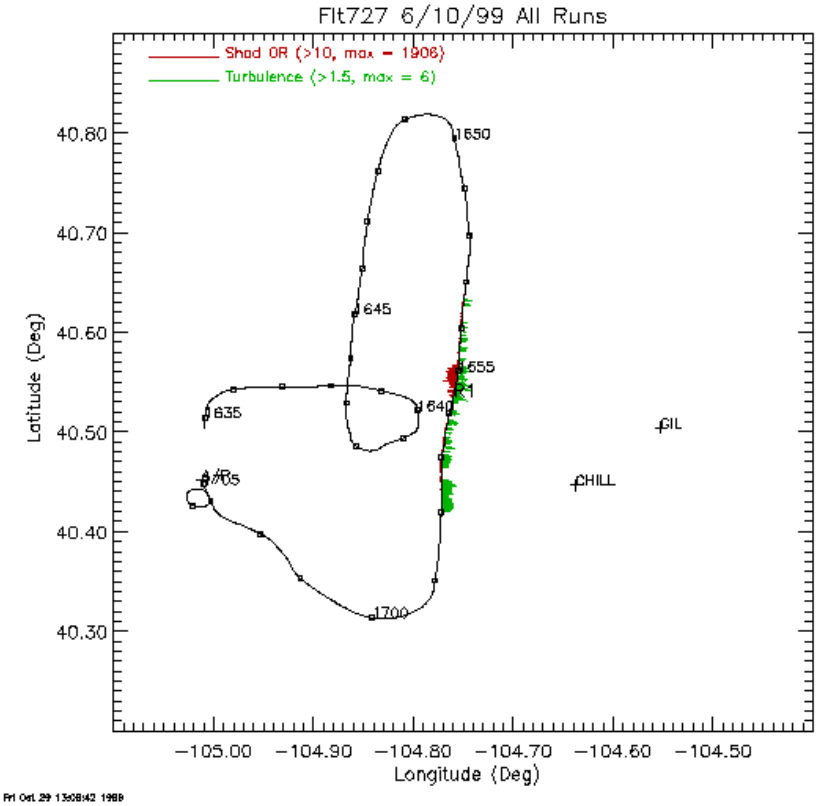
Flt727 6/10/99 All Runs
Shad OR (>10, max = 1906)
Turbulence (>1.5, max = 6)
40.80
40.70
40.60
40.50
40.40
40.30
Latitude (Deg)
1650
645
655
635
640
GIL
CHILL
1700
−105.00
−104.90
−104.80
−104.70
−104.60
−104.50
Longitude (Deg)

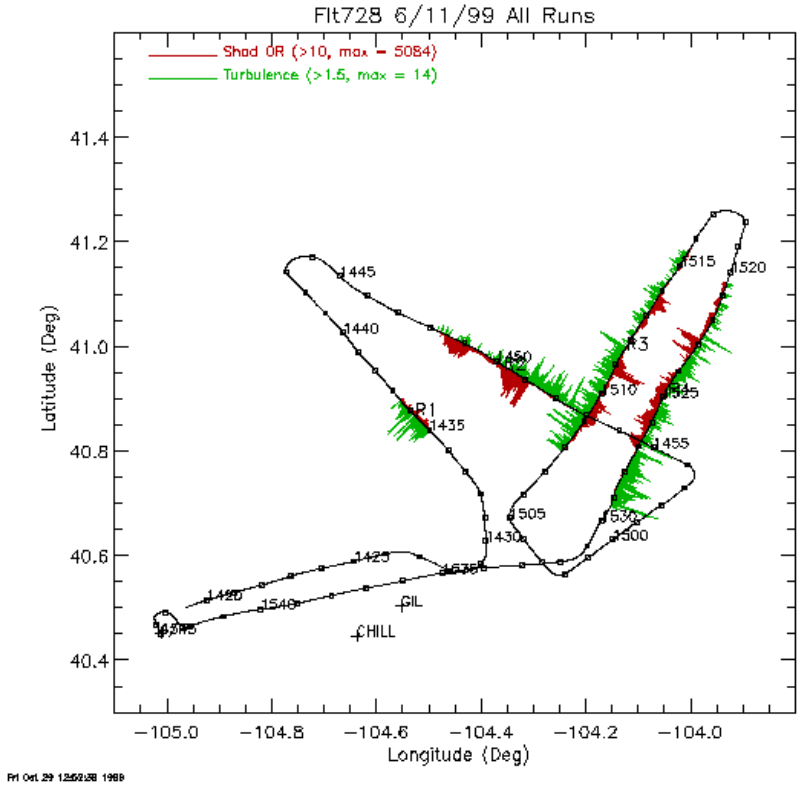
Flt728 6/11/99 All Runs
Shad OR (>10, max = 5084)
Turbulence (>1.5, max = 14)
41.4
41.2
41.0
40.8
40.6
40.4
Latitude (Deg)
1445
1515
1520
1440
R3
1510
R1
1435
1455
1505
1430
1425
1420
1540
GIL
CHILL
−105.0
−104.8
−104.6
−104.4
−104.2
−104.0
Longitude (Deg)

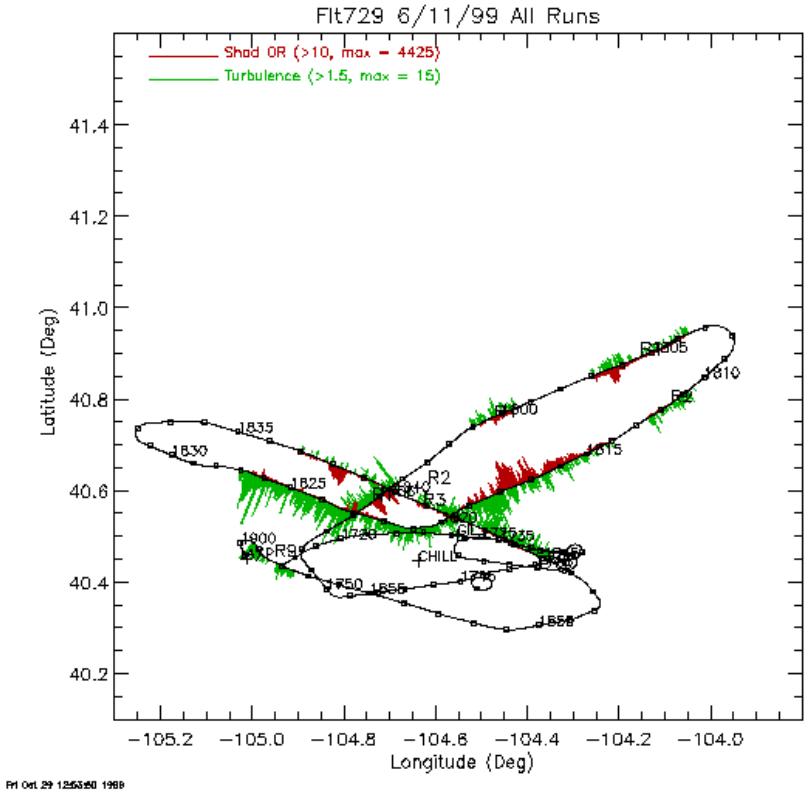
Flt729 6/11/99 All Runs
Shad OR (>10, max = 4425)
Turbulence (>1.5, max = 15)
Latitude (Deg)
Longitude (Deg)
41.4
41.2
41.0
40.8
40.6
40.4
40.2
−105.2
−105.0
−104.8
−104.6
−104.4
−104.2
−104.0
R2
CHILL
1835
1830
1825
1900
1750
1855
1858
1810
1815

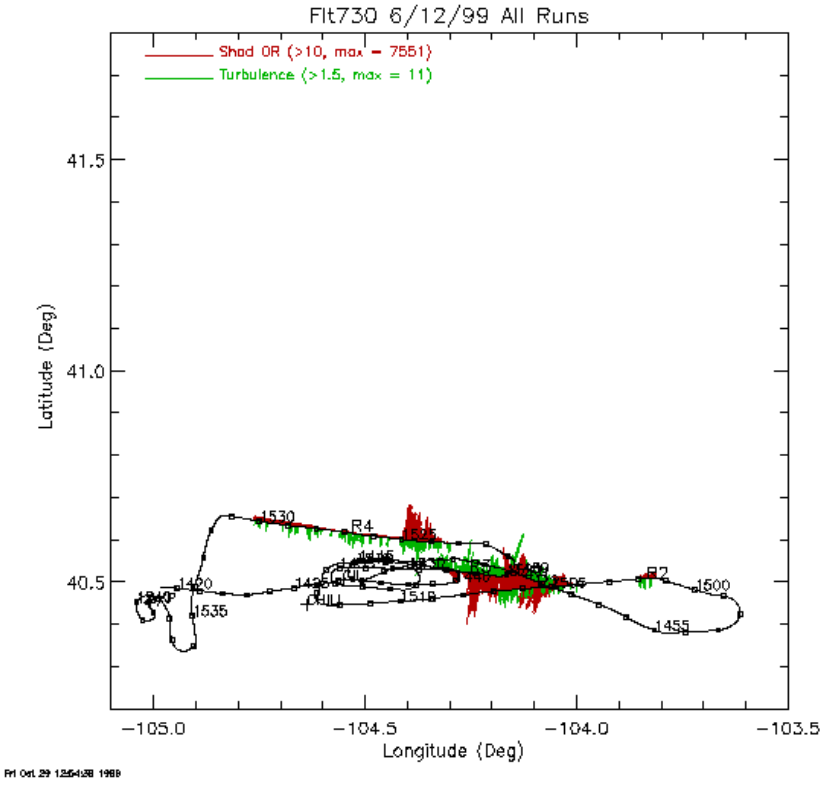
Flt730 6/12/99 All Runs
Shad OR (>10, max = 7551)
Turbulence (>1.5, max = 11)
Latitude (Deg)
Longitude (Deg)
41.5
41.0
40.5
−105.0
−104.5
−104.0
−103.5
R4
R2
CHILL
1530
1420
1535
1518
1500
1455

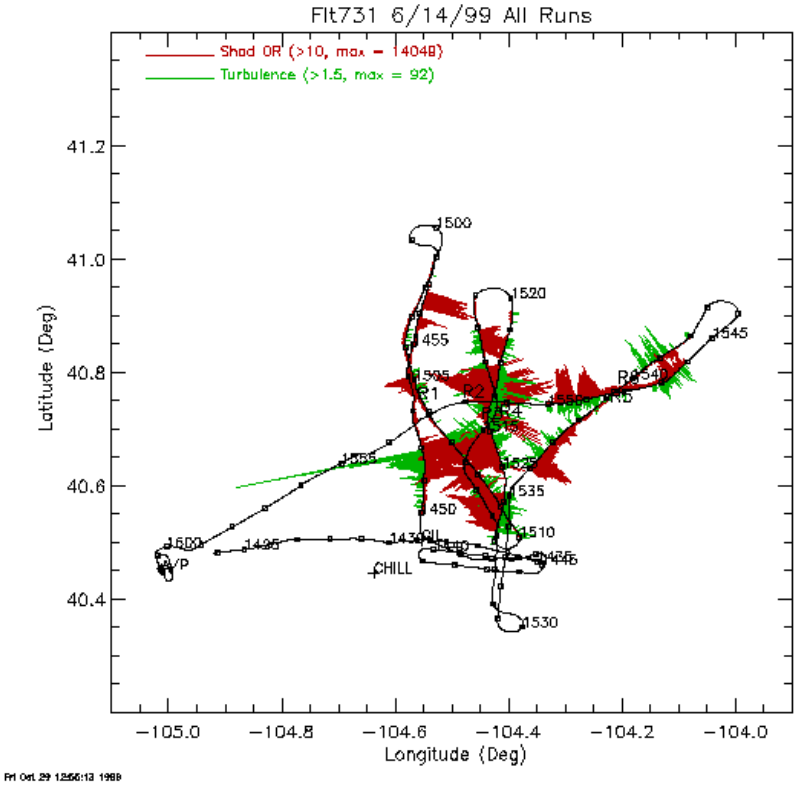
Flt731 6/14/99 All Runs
Shad OR (>10, max = 14048)
Turbulence (>1.5, max = 92)
Latitude (Deg)
Longitude (Deg)
41.2
41.0
40.8
40.6
40.4
−105.0
−104.8
−104.6
−104.4
−104.2
−104.0
1500
1520
1545
455
1535
450
1510
1530
1600
1430
CHILL
R1
R2
R3

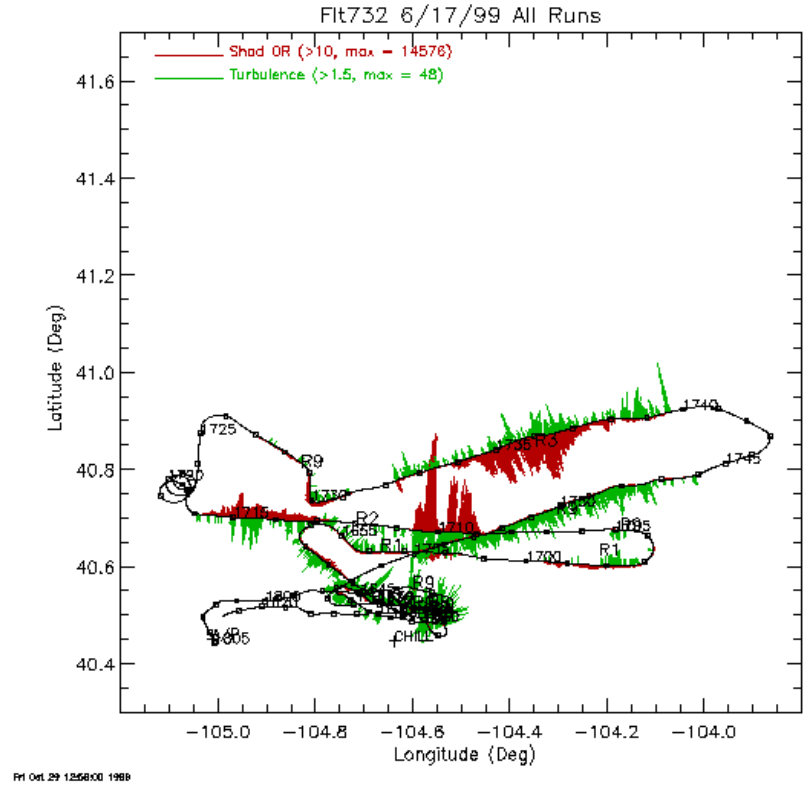
Flt732 6/17/99 All Runs
Shad OR (>10, max = 14576)
Turbulence (>1.5, max = 48)
Latitude (Deg)
Longitude (Deg)
41.6
41.4
41.2
41.0
40.8
40.6
40.4
−105.0
−104.8
−104.6
−104.4
−104.2
−104.0
725
1740
1745
1700
1705
CHILL
R1
R2
R3
R9

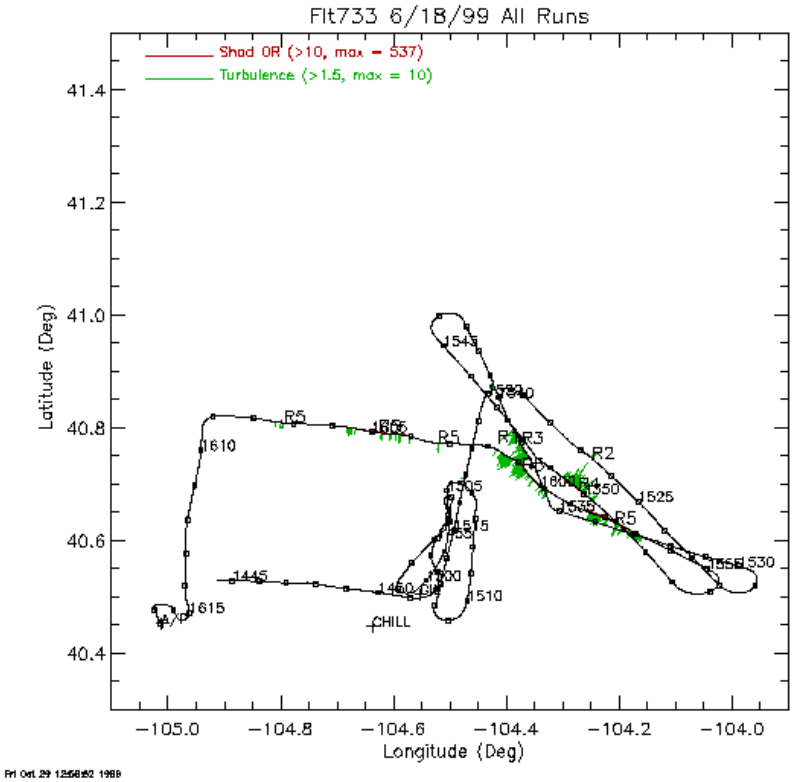
Flt733 6/18/99 All Runs
Shad OR (>10, max = 537)
Turbulence (>1.5, max = 10)
Latitude (Deg)
Longitude (Deg)
41.4
41.2
41.0
40.8
40.6
40.4
−105.0
−104.8
−104.6
−104.4
−104.2
−104.0
R5
R3
R2
1610
1615
1445
1510
1525
1530
CHILL

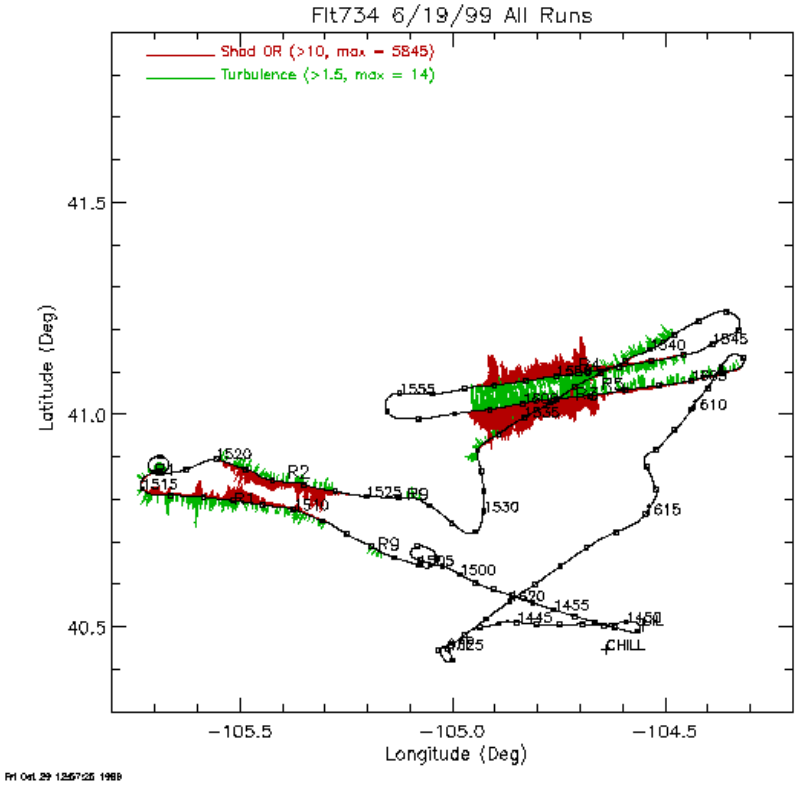
Flt734 6/19/99 All Runs
Shad OR (>10, max = 5845)
Turbulence (>1.5, max = 14)
Latitude (Deg)
Longitude (Deg)
41.5
41.0
40.5
−105.5
−105.0
−104.5
R2
R9
1515
1520
1525
1530
1555
1610
1615
1500
1455
1445
1450
CHILL

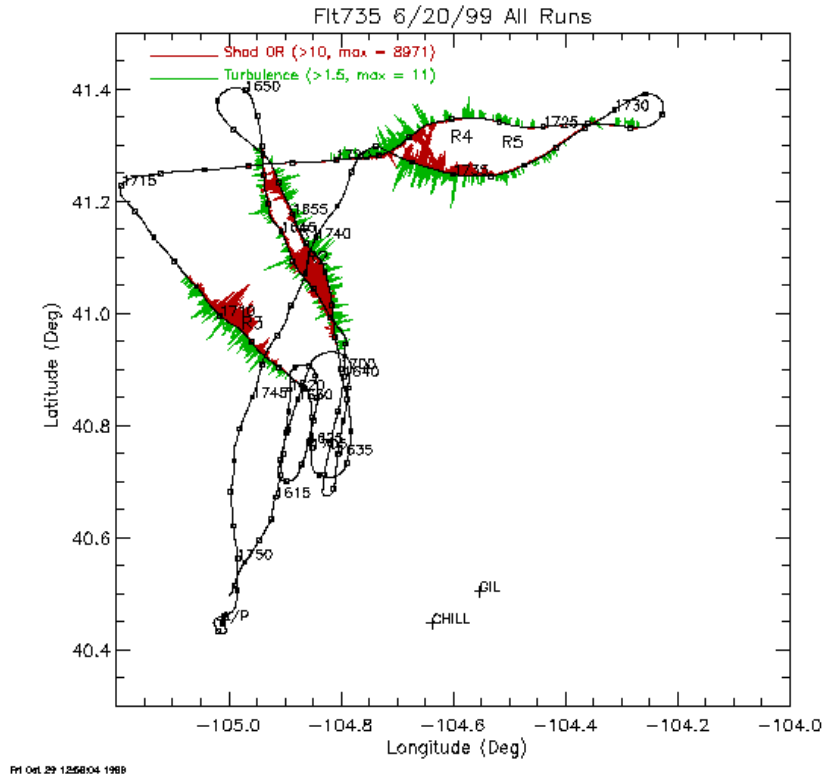
Flt735 6/20/99 All Runs
Shad OR (>10, max = 8971)
Turbulence (>1.5, max = 11)
1650
1730
1725
R4
R5
1715
1655
1645
1740
1745
1640
1635
1615
1750
GIL
CHILL
41.4
41.2
41.0
40.8
40.6
40.4
−105.0
−104.8
−104.6
−104.4
−104.2
−104.0
Latitude (Deg)
Longitude (Deg)

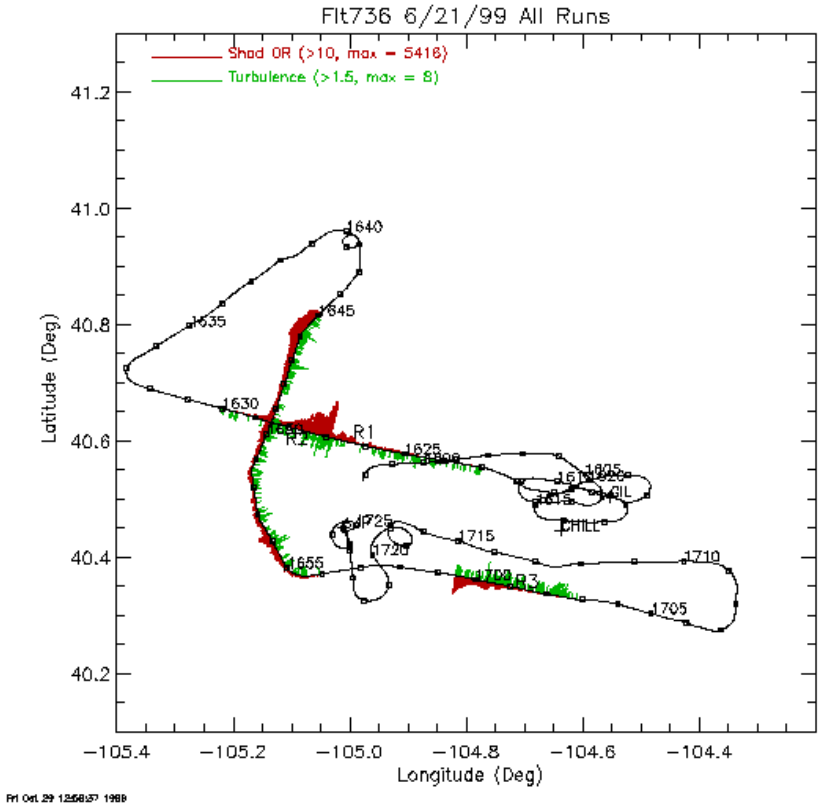
Flt736 6/21/99 All Runs
Shad OR (>10, max = 5416)
Turbulence (>1.5, max = 8)
1640
1645
1635
1630
R1
R2
1625
1725
1715
1720
1655
1710
1705
GIL
CHILL
41.2
41.0
40.8
40.6
40.4
40.2
−105.4
−105.2
−105.0
−104.8
−104.6
−104.4
Latitude (Deg)
Longitude (Deg)

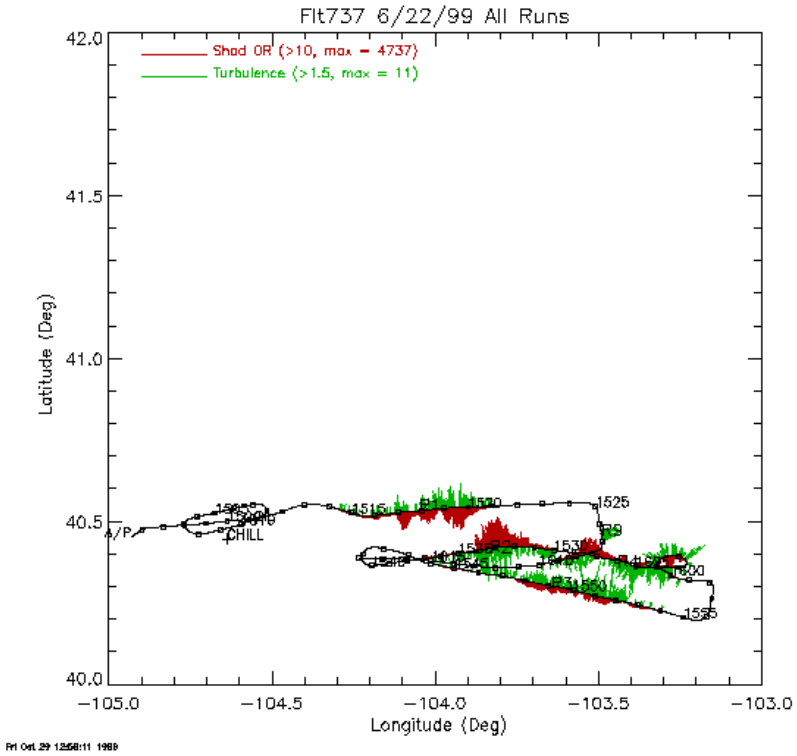
Flt737 6/22/99 All Runs
Shad OR (>10, max = 4737)
Turbulence (>1.5, max = 11)
42.0
41.5
41.0
40.5
40.0
Latitude (Deg)
−105.0
−104.5
−104.0
−103.5
−103.0
Longitude (Deg)
A/P
CHILL
1525
1535
Fri Oct 29 12:58:11 1999